Title
Role of sea surface temperature, Arctic sea ice and Siberian snow in forcing the atmospheric circulation in winter of 2012–2013

Journal
Climate Dynamics, 45(5-6)

ISSN
0930-7575

Authors
Peings, Yannick
Magnusdottir, Gudrun

Publication Date
2015-09-01

DOI
10.1007/s00382-014-2368-1

Clim Dyn
DOI 10.1007/s00382-014-2368-1

Role of sea surface temperature, Arctic sea ice and Siberian snow in forcing the atmospheric circulation in winter of 2012–2013

Yannick Peings · Gudrun Magnusdottir

Received: 23 June 2014 / Accepted: 6 October 2014

Abstract During the 2012–2013 winter, the negative phase of the North Atlantic Oscillation (NAO) predominated, resulting in a cold winter over Europe and northern Asia punctuated by episodes of frigid weather. This climate anomaly is part of a recent trend towards negative values of the NAO index that has occurred over recent winters. The negative trend of the NAO may be related to atmospheric internal variability but it may also be partly forced by slowly varying components of the climate system. In the present study, we investigate the influence of surface conditions on the atmospheric circulation for the 2012–2013 winter using an atmospheric global climate model. In particular, the role of low Arctic sea ice concentration, warm tropical/North Atlantic sea surface temperature and positive Siberian snow cover anomalies are isolated by prescribing them in a set of different numerical experiments. Our simulations suggest that each of these surface forcings favored a negative NAO during the 2012–2013 winter. In our model, the combined NAO response to tropical/North Atlantic SST, Arctic sea ice and Siberian snow anomalies accounts for about 30 % of the observed NAO anomaly. Different physical mechanisms are explored to elucidate the atmospheric responses and are shown to involve both tropical and extratropical processes.

Keywords Climate variability · North Atlantic Oscillation · Ocean-atmosphere interactions · Arctic sea ice · Siberian snow · 2012–2013 winter

Electronic supplementary material The online version of this article (doi:10.1007/s00382-014-2368-1) contains supplementary material, which is available to authorized users.

Y. Peings (✉) · G. Magnusdottir
Department of Earth System Science, University of California, Irvine, Irvine, CA 92697-3100, USA
e-mail: ypeings@uci.edu

1 Introduction

Recent winters have been characterized by a resurgence of extreme cold weather over the northern mid-latitudes (Jung et al. 2011; Maidens et al. 2013; Peterson et al. 2013; Slingo 2013; Ballinger et al. 2014). Episodes of anomalously cold temperature and snowfall have hit some regions of Europe, Asia and North America with strong socio-economic consequences (e.g., the 2009/2010 cold winter over Europe/eastern US, the deadly cold spell of February 2012 over central Europe, frigid temperature in March 2013 over the UK, the cold snap of early January 2014 over the eastern US). These climatic anomalies have raised questions as to what may be driving them as they are somewhat at odds with the long-term expected consequences of global change including the projected decay of cold extremes (Collins et al. 2013). Several studies have suggested that the recent acceleration of Arctic sea ice retreat is a possible driver for the resurgence of cold weather episodes (Francis et al. 2009; Petoukhov and Semenov 2010; Liu et al. 2012; Tang et al. 2013). Francis and Vavrus (2012) proposed the following mechanism: with Arctic sea-ice loss and the associated Arctic amplification (Serreze et al. 2009), the northward temperature gradient in winter is decreased resulting in a slower jet stream and thus slower moving weather systems so that cold anomalies can linger. However, this mechanism has been challenged since it is metric-dependent and hardly detectable in the observations (Screen and Simmonds 2013; Barnes 2013). Moreover, recent cold air outbreaks are not unprecedented (Cellitti et al. 2006; Guirguis et al. 2011) and are consistent with the strong natural variability inherent to the climate system (Wallace et al. 2014). An extensive review of the recent findings concerning a link between the Arctic sea ice decline and the mid-latitude winter weather is given in Vihma (2014).

Regardless of the possible influence of Arctic amplification, the resurgence of cold winters in the northern mid-latitudes is consistent with the recent trend towards the negative polarity of the North Atlantic Oscillation (NAO) and Northern Annular Mode (NAM), that followed two decades of positive trend in the 1980s and 1990s (Cohen et al. 2012). The NAO is a climate pattern that describes the seesaw in atmospheric pressure in the North Atlantic basin between the Icelandic low and the Azores high. The NAM is highly correlated with the NAO but describes the hemispheric teleconnection between the atmospheric mass of the Arctic and the northern mid-latitudes (Thompson and Wallace 1998). Large anomalies in surface temperature and precipitation across North America and Eurasia are associated with the NAO/NAM, including colder temperature in mid-latitudes during the negative NAO/NAM polarity (Hurrell and van Loon 1997). Although the NAO/NAM is an internal mode of atmospheric variability, it can be modulated by slowly varying boundary conditions. There is abundant literature about NAO/NAM predictability and the influence of boundary forcings on its intraseasonal to multidecadal variability. In particular, sea surface temperature anomalies (e.g., Czaja and Frankignoul 1999; Peng et al. 2002; Toniazzo and Scaife 2006; Deser et al. 2007), Arctic sea ice anomalies (e.g., Alexander et al. 2004; Magnusdottir et al. 2004; Deser et al. 2010; Kumar et al. 2010; Semmler et al. 2012) and Eurasian snow cover anomalies (e.g., Cohen et al. 2007; Fletcher et al. 2009; Peings et al. 2012) have been suggested as potential drivers of NAO/NAM variability. The NAO/NAM is also closely tied to the stratospheric circulation (Douville 2009), as well as possibly influenced by solar forcing and volcanic activity (Gray et al. 2013; Fischer et al. 2007; Ineson et al. 2011). Seasonal forecast systems have recently improved their skill in predicting the NAO/NAM and its associated impacts (Scaife et al. 2014; Kang et al. 2014). This improvement gives interesting possibilities for providing skillful seasonal climate forecasts months ahead. However, the key sources of predictability of the NAO/NAM are still only partially understood. Idealized studies are therefore important for providing improved physical understanding of the large-scale teleconnections and for identifying additional sources of predictability.

In a previous study (Peings and Magnusdottir 2014a), we specifically investigated the impact of recent Arctic sea ice anomalies on the Northern Hemisphere (NH) wintertime atmospheric circulation using the Community Atmospheric Model Version 5 (CAM5). Our numerical experiments revealed only a small response of the winter-mean atmospheric circulation to the sea ice forcing (in line with Screen et al. 2013) and little impact on the increase of extreme cold weather in the mid-latitudes, except over Asia (in line with Honda et al. 2009). Another potential driver of the recent atmospheric cold spells in the NH is the Atlantic Multidecadal Oscillation (AMO). The AMO depicts the basin-scale multidecadal variability of the North Atlantic sea surface temperature (SST), with periods of anomalous cold SST anomalies alternating with periods of anomalous warm SST anomalies (Kerr 2000). This cycle has a period of about 60–70 years in SST observations and is also referred as Atlantic Multidecadal Variability since it is difficult to assess whether it has a stationary periodicity (as the observational record is too short to contain more than 2 cycles). The AMO had a negative polarity until the late 1990's when it reversed to a positive polarity. Recent studies have suggested that the AMO is able to significantly modulate the NAO in winter, based on climate model simulations (Msadek et al. 2011; Kavvada et al. 2013; Omrani et al. 2014; Peings and Magnusdottir 2014b). They found that the positive AMO is able to force a significant negative NAO pattern in the atmosphere. This inverse AMO-NAO relationship, that is also identified in the twentieth Century Reanalysis (20CR) over 1901–2010 (Peings and Magnusdottir 2014b), suggests that the current positive polarity of the AMO promotes the recent trend towards a negative NAO and more severe winter weather in Europe and the eastern US.

This paper is an extension of our recent papers (Peings and Magnusdottir 2014a, b). Here we investigate the role of surface boundary conditions on the wintertime atmospheric circulation, using the 2012–2013 winter as a case study. Our aim is to characterize the respective and combined influences of tropical/North Atlantic SST, Arctic sea ice and Siberian snow cover anomalies on the anomalous atmospheric circulation of this specific winter. We selected the 2012–2013 winter based on the following observations. On average, this winter (December to March, DJFM) was characterized by a strong negative NAO pattern that induced cold surface temperature anomalies in the northern mid-latitudes (Sect. 3.1). The value of the DJFM NAO index is −1.97 according to the station-based index of Hurrell, −1.66 using the index that is computed from an Empirical Orthogonal Function (EOF) analysis (source https://climatedataguide.ucar.edu/climate-data/hurrell-north-atlantic-oscillation-nao-index-station-based). Extreme cold temperature was recorded over Europe, for instance in the UK where the month of March was the coldest since 1962 (Slingo 2013). Meanwhile, the sea ice extent in the Arctic was anomalously low in fall/winter 2012–2013 following the lowest extent ever recorded by satellite in September (source https://nsidc.org). Moreover, warm SST anomalies were present in the tropical and North Atlantic in line with the current polarity of the AMO (Peings and Magnusdottir 2014b) and the Siberian snow cover extent was greater than normal in fall 2012 (see http://climate.rutgers.edu/snowcover for monthly departure charts). Therefore, the

2012–2013 winter provides an ideal setting for exploring the influence of each of the three potential surface forcings on the wintertime NH climate, and to estimate the fraction of the negative NAO signal that was forced by them.

For this purpose, several experiments are performed with CAM5 in order to separate the role of each forcing mechanism and estimate its relative impact on the anomalous atmospheric circulation observed during the 2012–2013 winter. The model and experiments are described in Sect. 2. Section 3 presents the atmospheric response in the experiments and discusses physical mechanisms. Finally, results are summarized and discussed in the conclusion.

2 Methods

2.1 Observational dataset

Sea surface temperature (SST) and sea ice concentration (SIC) that are imposed in CAM5 come from the HadISST dataset (Rayner et al. 2003) that is of 1° spatial resolution. Sea ice is retrieved from various sources of digitized sea ice charts and passive microwave imagery. National Centers for Environmental Prediction/National Center for Atmospheric Research (NCEP/NCAR) reanalysis (Kalnay et al. 1996) is used for describing the atmospheric circulation of the 2012–2013 winter. Precipitation anomalies are obtained from the Global Precipitation Climatology Project (GPCP) dataset (Adler et al. 2003). This monthly precipitation dataset combines in-situ observations and satellite precipitation data into a 2.5°×2.5° global grid from 1979 to present.

2.2 Experimental design

The numerical experiments are performed with an atmospheric general circulation model (AGCM), the Community Atmospheric Model version 5 (CAM5) developed at the National Center for Atmospheric Research (NCAR). CAM5 is the atmospheric component of the Community Earth System Model (CESM, Neale et al. 2011). Compared to the previous version, it includes new physics and a new aerosol scheme. The Community Land Model (CLM 4.0) is used as a land surface model. The horizontal resolution selected in this study is 1.9° latitude and 2.5° longitude. Concerning the vertical resolution, CAM5 is a low-top model with 30 vertical levels and a lid around the 3 hPa pressure level. SST and sea ice concentration are prescribed to the model after a linear interpolation of monthly values. Greenhouse gas and aerosol concentrations are representative of present-day conditions (year 2000).

The control experiment ("CTL") is a 50-year simulation forced with the repeating 1979/2008-average annual cycle of SST/SIC from HadISST. Five perturbation experiments are conducted. Each perturbation experiment consists of a 50-member ensemble that is paired to CTL such that they only differ by the lower boundary conditions (SST, SIC or Siberian snow). Each ensemble member is started from different initial conditions corresponding to October 1st of a particular year in CTL. Ensemble member experiments starting on October 1st are run until the following May 31st to span both the winter and spring seasons. However, we only explore the wintertime atmospheric response in the present study. The design of the experiments is described below and they are summarized in Table 1. Figure 1 shows the surface forcing that is imposed in winter (DJFM average) in each of the 5 perturbation experiments.

- GLOB is forced with the global 2012–2013 SST and SIC (Fig. 1a). It explores the role of the global SST/SIC anomalies observed during the 2012–2013 winter on the atmospheric circulation. SST and SIC anomalies modulate the overlying atmosphere through surface energy flux exchanges (radiative and turbulent heat fluxes). Warm SST anomalies and less sea ice result in a gain of energy by the atmosphere through an increase in air-sea heat flux. Less sea ice decreases the surface albedo and

Table 1 Description of the experiments

Name	Description	Forcing included
CTL	50-year control experiment with climatological SST/SIC (annual cycle of SST/SIC averaged over the 1979–2008 period)	NA
GLOB	50 Members forced with the 2012–2013 global SST and SIC	Global SST/SIC
GLOBSN	Same as GLOB plus a 100 mm snow water equivalent anomaly imposed on the 1st of October over Siberia	Global SST/SIC + Siberian snow
NATL	50 Members forced with the 2012–2013 SST over the tropical and North Atlantic (35°S–85°N), and climatological SST/SIC elsewhere	Tropical/North Atlantic SST
ASIC	50 Members forced with the 2012–2013 Arctic sea ice concentration and climatological SST/SIC elsewhere	Arctic sea ice concentration
OTHER	50 Members forced with the 2012–2013 SST outside of the North Atlantic and Arctic, and climatological SST/SIC over North Atlantic/Arctic.	SST outside of North Atlantic/Arctic (Pacific, Indian and south Atlantic ocean)

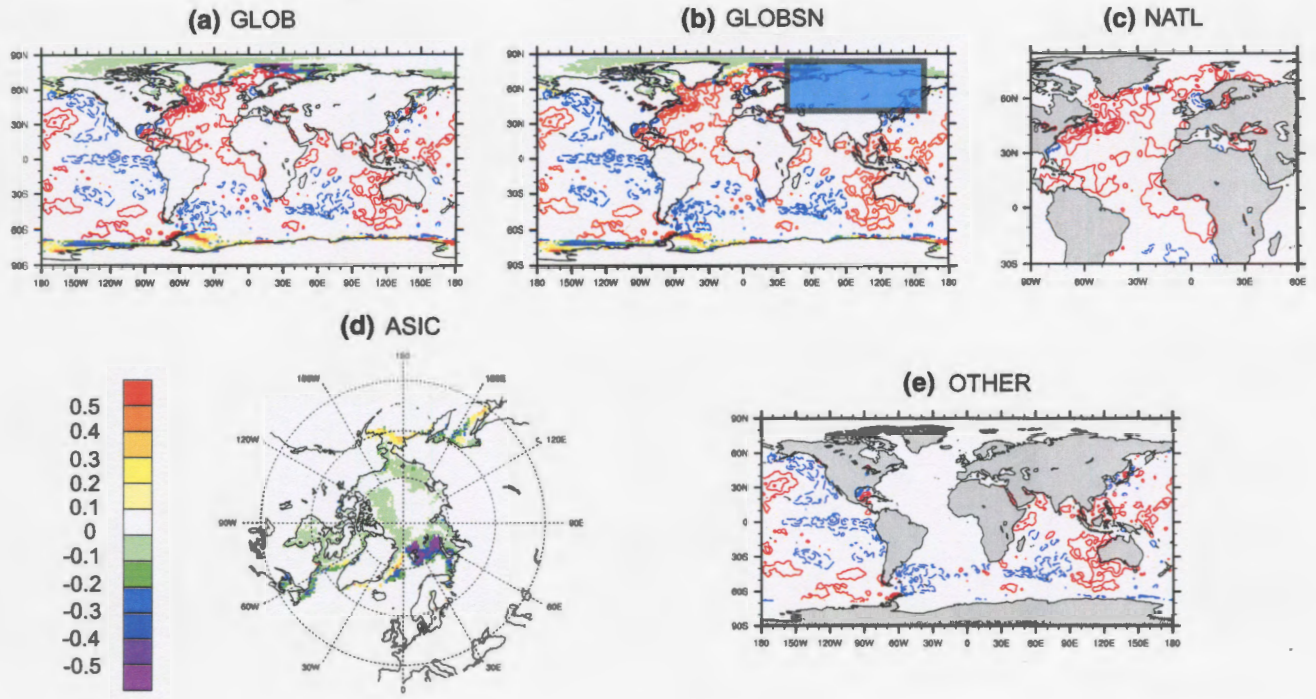

Fig. 1 Surface forcing prescribed to the model for each perturbation experiment (compared to CTL): **a** SST and SIC anomalies in GLOB; **b** SST and SIC anomalies in GLOBSN, as well as area of the initial snow anomaly (100 mm equivalent water) over Siberia; **c** SST anomalies in NATL; **d** sea ice anomalies in ASIC; **e** SST anomalies in OTHER. The contour interval for SST is 0.4 K (*red contours* for positive anomalies, *blue* for negative anomalies, zero contour ommited). Sea ice anomalies are expressed in fraction of covered area (see *color bar*)

warms the upper layer of the ocean as more solar radiation reaches the ocean surface. The turbulent heat fluxes and upward longwave radiative flux are increased, resulting in a warming of the lower troposphere (Deser et al. 2010). While sea ice anomalies are maximum in summer, their impact on the surface energy budget is stronger in fall/winter (Deser et al. 2010; Screen et al. 2013; Peings and Magnusdottir 2014a). Since the ocean is not interactive in our model, we take into account the change of SST associated with sea ice anomalies by imposing the 2012–2013 SST anomalies where the sea ice is substantially modified (see Peings and Magnusdottir 2014a for further details on this method).

- NATL is forced with the 2012–2013 SST over the tropical and North Atlantic (35°S–85°N). Climatological SST/SIC of 1979–2008 are prescribed everywhere else. This experiment allows us to isolate the role of the tropical and North Atlantic SST in forcing the atmospheric circulation of the 2012–2013 winter.
- ASIC is forced with the 2012–2013 sea ice concentration in the Arctic and climatological SST/SIC everywhere else. This experiment isolates the impact of the Arctic sea ice anomalies on the atmospheric circulation. To take into account the SST changes associated with sea ice anomalies, we use the same method as for GLOB.
- OTHER is forced with the 2012–2013 SST outside of the tropical/North Atlantic and Arctic oceans. Climatological SST/SIC are prescribed over the tropical/North Atlantic and the Arctic. This experiment aims to determine the influence of SST anomalies that are outside the tropical/North Atlantic and Arctic oceans.
- GLOBSN is an additional experiment that was designed to estimate the impact of an excess of snow over Siberia, as observed in fall/winter 2012–2013. It is similar to GLOB (2012–2013 SST/SIC everywhere) except for the prescription of a snow anomaly on the 1st of October over Siberia. At the time of the study, snow cover data were not available for the 2012–2013 season so we decided to impose an arbitrary amount of snow over Siberia to simulate an excess of snow (100 mm of snow water equivalent in the [40N/80N;40E/160E] sector). Each ensemble member of the experiment is initialized with the same snow anomaly, and the snow evolves freely afterwards. The amplitude of the snow anomaly has been chosen to be consistent with previous sensitivity studies that explored the impact of Siberian snow (Fletcher et al. 2009; Peings et al. 2012). The snow anomaly is imposed in fall, but persists through winter and spring. Therefore, GLOBSN has a larger albedo and colder surface temperature over Siberia from October to May.

In the following, the forcing induced by the SST, SIC or snow anomalies that is imposed in the experiments is referred to using the name of the experiment (for instance, "GLOB" refers to the forcing induced by the global SST and SIC anomalies).

2.3 Statistical tools and physical diagnostics

Cold days are defined at each grid point as days below the 10th percentile of the daily temperature distribution. Cold-day anomalies are expressed in percentage, as a departure from the climatological percentage of cold days (10 %, by construction). For example, an anomaly of 5 % means that during this particular winter 15 % of the days were cold days.

The eddy transient activity is characterized using the standard deviation of the bandpass filtered daily geopotential height at 500 hPa (Z500). A 2–6 day band pass Lanczos filter (Duchon 1979) is applied to the daily Z500 anomalies to keep only the synoptic variability.

The E-vector describes the transient eddy forcing upon the local time-mean flow (Hoskins et al. 1983). It is computed from the horizontal components of the wind, after filtering with a 2–6 days bandpass Lanczos filter: $E = \left(\overline{v'^2 - u'^2}, \overline{-u'v'}\right)$. E is in the direction of the group velocity of the transient eddies relative to the local time-mean flow. The divergence of E depicts the eddy-induced acceleration of the horizontal flow due to barotropic processes.

The North Atlantic weather regimes are obtained from daily anomalies of Z500 using a k-mean algorithm. To reduce the computational time, the k-mean clustering algorithm is applied to the first 15 principal components of the anomalous daily Z500. Four weather regimes are retained for the classification (Vautard 1990), which is performed one hundred times for testing the robustness of the cluster partition. Then each winter day is attributed to one of the four centroids of the k-mean partition according to a spatial correlation criterion ($r > 0.25$ between the anomaly and the centroid) and a duration criterion (one regime must last at least 3 days to be selected as a regime occurrence).

3 Results

3.1 Response in sea-level pressure and the NAO

Figure 2 compares the winter SLP response in each perturbation experiment to the observed anomalies of the 2012–2013 winter (Fig. 2a). Note that in most of the following figures the contour interval is smaller for the simulations than for observations, since the model response is always less than the observed anomaly. This result is to be expected given that we are comparing ensemble means of model experiments to a single season of observations. The spatial correlation between the observed signal and the response is given in the upper right corner of the plots. The first number gives the correlation with the total pattern of the response (contours), the second number gives the correlation with the statistically significant part only (color shading). The spatial correlation is a measure of the agreement between the ensemble-mean pattern of each experiment vs the observed anomalies for the 2012–2013 winter (NCEP). Since we are particularly interested in the response of the NAO, the pattern of the NAO in our model is superimposed in Fig. 2b (red contours). It is the first EOF of the DJFM SLP from CTL in the North Atlantic sector. Each of the SLP responses of Fig. 2 are regressed onto this NAO pattern to estimate the anomaly of the NAO index that is associated with the SLP response. The ensemble-mean NAO index anomalies are summarized in Table 2 and compared to the observed value for the 2012–2013 winter (−1.66, from EOF method).

GLOB (Fig. 2b) realistically simulates the observed low in the North Atlantic and the observed high over the North Pacific, with a rather high amplitude of the signal in both cases (still approximately 2 times smaller than NCEP). Unlike NCEP, the low in the North Atlantic does not extend over Europe, but the main discrepancy is the response over the Arctic. The response is opposite to NCEP with significant negative values of SLP instead of large positive anomalies. This signal is equivalent barotropic since it is also visible in 500 hPa geopotential height (not shown). The agreement with NCEP is better in the Arctic when the Siberian snow anomaly is added in the model (GLOBSN, Fig. 2c). Indeed, the negative SLP anomalies are less intense and even become positive in the North Atlantic sector of the Arctic such that a negative-NAO pattern emerges. This is illustrated by the value of the NAO index that decreases from −0.13 in GLOB to −0.5 in GLOBSN (Table 2). This response to the snow forcing supports the documented inverse relationship between the Siberian snow and the NAO/NAM (Cohen et al. 2007; Fletcher et al. 2009; Peings et al. 2012). In agreement with previous studies, an excess of Siberian snow in our model promotes higher pressures over the Arctic and thereby negative values of the NAO.

NATL (Fig. 2d) illustrates the effect of the tropical and North Atlantic SST anomalies. They play an important role in the low pressure anomaly over the North Atlantic, with an extension over southern Europe and North Africa in line with the observed response. NATL also induces a significant positive anomaly in the North Pacific that is consistent with NCEP. This remote response suggests the existence of an Atlantic-Pacific teleconnection. As in GLOB, significant low-pressure anomalies are found in the Arctic, which is

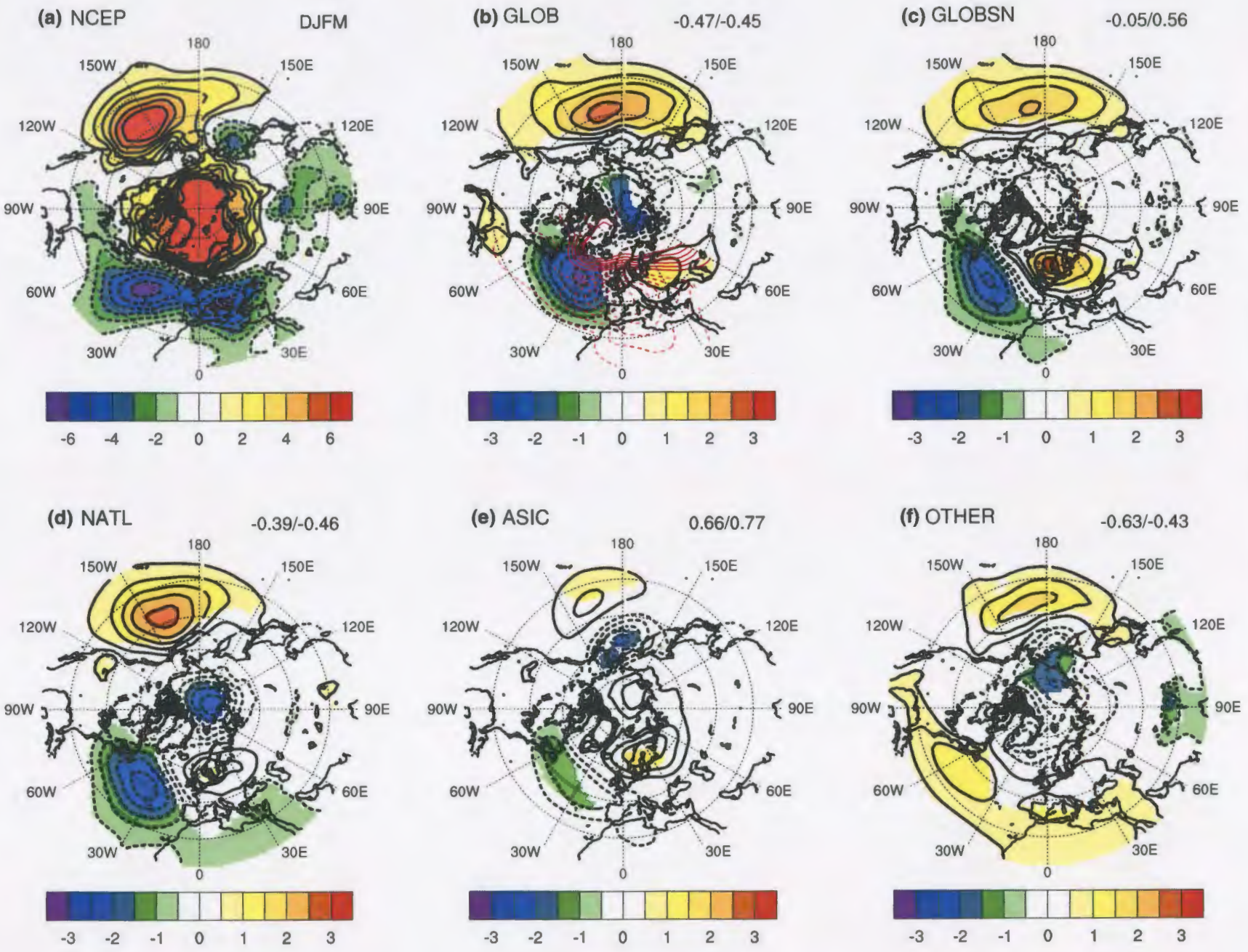
(a) NCEP
DJFM
(b) GLOB
-0.47/-0.45
(c) GLOBSN
-0.05/0.56
(d) NATL
-0.39/-0.46
(e) ASIC
0.66/0.77
(f) OTHER
-0.63/-0.43
180
150W
150E
120W
120E
90W
90E
60W
60E
30W
30E
0
-6 -4 -2 0 2 4 6
-3 -2 -1 0 1 2 3

◀**Fig. 2** **a** Observed sea level pressure anomalies (hPa) during the 2012-2013 winter (DJFM average). **b** Response of the DJFM SLP in GLOB (*contours*). Anomalies significant at the 95 % confidence level are *shaded*. The spatial correlation between the model response and the observed anomaly is indicated on the top-right of the plot (total response/significant part only). **c** Same as **b** for GLOBSN. **d** Same as b for NATL. **e** Same as **b** for ASIC. **f** Same as **b** for OTHER. The NAO pattern (EOF of DJFM SLP in the North Atlantic domain) is superimposed in *red contours* (1 hPa contour interval) in **b**

opposite to NCEP. This result is interesting in light of Peings and Magnusdottir (2014b) that showed a positive SLP response over the Arctic associated with the positive AMO polarity. The opposite response in the Arctic illustrates the difference of imposing decadal SST anomalies vs seasonal SST anomalies. In Peings and Magnusdottir (2014b), the SST anomalies due to the AMO that were used to force the model were low-pass filtered to keep only the multidecadal variability of SST. This signal is considered driven largely by ocean dynamics (Eden and Jung 2001; Gulev et al. 2013). In the present study, we impose seasonal SST anomalies that include short-term variability forced by the atmosphere through heat flux exchanges (Bjerknes 1964). Consequently, the response of the SST to the atmospheric anomaly that we try to reproduce is included in the experiment, leading to a different pattern of SST anomalies. Compared to Peings and Magnusdottir (2014b, Fig. 1b), the SST anomalies of NATL are confined to the Gulf stream region in the western part of the basin. This is especially true in the 30°N–60°N latitudinal band where SST anomalies had a great influence on the storm track activity in Peings and Magnusdottir (2014b). Also, their SST forcing stopped at the equator while NATL includes some southern tropical SST anomalies from equator to 35°S. In addition to the different pattern of SST anomalies, two other factors may also explain the different response between the two studies. First, Peings and Magnusdottir (2014b) compared two perturbation experiments directly (positive AMO vs negative AMO) without using a control run as a reference. Secondly, Peings and Magnusdottir (2014b) also included the decadal SIC anomalies associated with the AMO (although the SIC anomalies were quite small and had probably little influence on the results).

ASIC gives a remarkably good representation of the observed pattern of SLP anomalies over the NH (Fig. 2e), as suggested by the high spatial correlations (R = 0.66/0.77) and the value of the corresponding NAO index (−0.57, Table 2). Unlike NATL, ASIC shows a high over the Arctic (Fig. 2e) that is consistent with NCEP and suggests that a competing mechanism may exist in this region between the response to NATL and ASIC. However, the response is of small amplitude with only limited area of statistical significance. This experiment supports previous findings that have identified a negative NAO/NAM pattern in response to a decrease of Arctic sea ice (Magnusdottir et al. 2004; Alexander et al. 2004; Deser et al. 2010) while confirming the weak amplitude of the signal when the recent Arctic sea ice anomalies are prescribed in an AGCM (Screen et al. 2013; Peings and Magnusdottir 2014a).

OTHER illustrates the impact of the SST anomalies from every region of the globe except the tropical/North Atlantic and the Arctic. It mainly includes the influence of the Pacific and Indian oceans, and in particular the impact of tropical Pacific SST that is known to play an important role in the global atmospheric variability through remote teleconnections (e.g., Horel and Wallace 1981). The 2012–2013 winter was characterized by a moderate La Nina signal in the tropical Pacific (see Fig. 1). Although the ENSO-NAO relationship is unclear, La Nina is often associated with a positive-NAO pattern in late winter, both in observations and climate models (Brönnimann 2007). Consequently, the strong negative NAO that was observed during the 2012–2013 winter was likely unrelated to the La Nina-SST anomalies in the tropical Pacific. In line with the ENSO-NAO linkage in the literature, the SLP response in OTHER (Fig. 2f) is reminiscent of the positive NAM/NAO, with negative spatial correlations of −0.63/−0.43 with the observed anomaly and a corresponding positive value of the NAO index (0.61, Table 2). The response is thus opposite to NCEP, except in the North Pacific where positive SLP anomalies are found. Assuming that the effect of the different surface forcings are additive (with little non-linear interactions between them), OTHER probably counteracts a negative NAO response forced in NATL, ASIC and GLOBSN. Without OTHER, the negative NAO response would be greater in GLOB and GLOBSN. This is illustrated in Fig. 3a that displays the SLP difference between GLOBSN and OTHER. Under the assumption that the

Table 2 Amplitude of the DJFM NAO index in each experiment compared to the observed NAO index

	Winter 2012–2013	GLOB	GLOBSN	NATL	ASIC	OTHER	GLOBSN-OTHER
NAO index anomaly	−1.66	−0.13	−0.5	−0.34	−0.57	0.61	−1.11
NAO regimes frequency anomaly (%)	39	10	17	11	12	−7	24

First row is for the NAO index (EOF-based index of Hurrel for observations, regression of the SLP response onto the NAO pattern for the simulations). Second row is for the combined anomaly in frequency of the NAO regimes, in % (sum of the anomalous frequencies of the NAO− and NAO+ regimes)

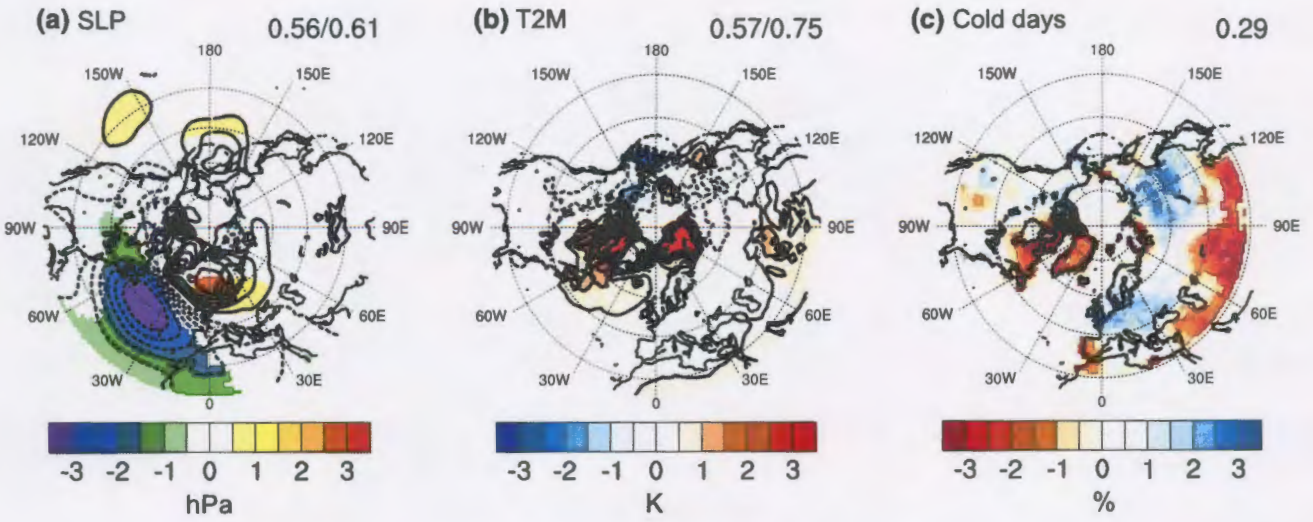

Fig. 3 Combined winter (DJFM) response to North Atlantic SST, Arctic sea ice and Siberian snow (estimated by computing the difference between GLOBSN and OTHER) : **a** for sea level pressure (hPa); **b** for 2-m temperature (K); **c** for the percentage of cold days (%). In **a**, **b**, the response is shown in contours and anomalies significant at the 95 % confidence level are shaded. The spatial correlation between the model response and the observed anomaly are indicated on the *top-right* of the plot (total response/significant part only)

response to the different forcings is linear, it illustrates the impact of NATL, ASIC and Siberian snow anomalies alone (without the impact of OTHER). In GLOBSN-OTHER, the response is more consistent with observations both in amplitude and spatial pattern. The value of the NAO index is −1.11 (Table 2) and the spatial correlations are higher than in GLOBSN-CTL (Fig. 2c). There is no evidence that demonstrates that the response of OTHER is less realistic than the response of GLOB, GLOBSN, NATL and ASIC. However, it is possible that CAM5 is too sensitive to the tropical Pacific forcing. If that is the case, the damping of the negative NAO by OTHER would be unrealistic and would lead to an underestimated impact of NATL, ASIC and Siberian snow. We cannot answer this question in the present study since determining the character of the ENSO-NAO teleconnection in CAM5 requires some additional experiments forced with interannual SST variability. Nonetheless, our experiments suggest that NATL, ASIC and the Siberian snow have favored the observed negative NAO of the 2012–2013 winter, while OTHER acted in the opposite way. In our simulations, the combined NAO response to NATL, ASIC and the Siberian snow represents about 30 % of the observed negative NAO anomaly (−0.5 compared to −1.66), and up to 60 % when OTHER is removed (−1.11 compared to −1.66).

The regression method of Table 2 gives an estimate of the winter-mean value of the NAO index. In order to examine this response at the intraseasonal time scale and to discuss its importance compared to atmospheric internal variability, we use the weather regime decomposition method (described in Sect. 2c). The North Atlantic weather regimes represent the typical synoptic-scale atmospheric patterns over the North Atlantic basin. Four weather regimes are commonly identified as representing a large part of the wintertime atmospheric variability in this region: the positive NAO (also called Atlantic low), the negative NAO, the Blocking and the Atlantic ridge regime (Cassou 2008). The weather regime decomposition has been applied to NCEP reanalysis over the 1948–2013 period and to our six experiments. The observed/simulated centroids of each regime are shown in the supplementary material (Fig. S1). The spatial patterns of the weather regimes are realistic in CAM5, as well as the climatological frequency of each regime. The weather regimes approach is helpful for determining the linearity of the NAO response (by isolating the response of the positive polarity from the response of the negative polarity) and it also accounts for the response of the Blocking and Atlantic ridge atmospheric patterns that are distinct from NAO variability.

Figure 4 displays for each simulation the distribution of wintertime frequencies of the four regimes. The distribution is depicted using a boxplot-whisker representation, with the mean of the distribution indicated by a red diamond. The frequency of each regime for the 2012–2013 winter is given at the bottom of Fig. 4 with climatology in parentheses. In line with the seasonal anomaly, the NAO− regime was predominant (47 %, compared to 22 % in climatology), while the NAO+ was present only 9 % of the time (compared to 23 % in climatology), corresponding to a combined (negative + positive) anomalous frequency of the NAO of 39 %. The Atlantic Ridge frequency was also anomalously low (−6 %) and the Blocking regime was close to climatology (2 % above mean).

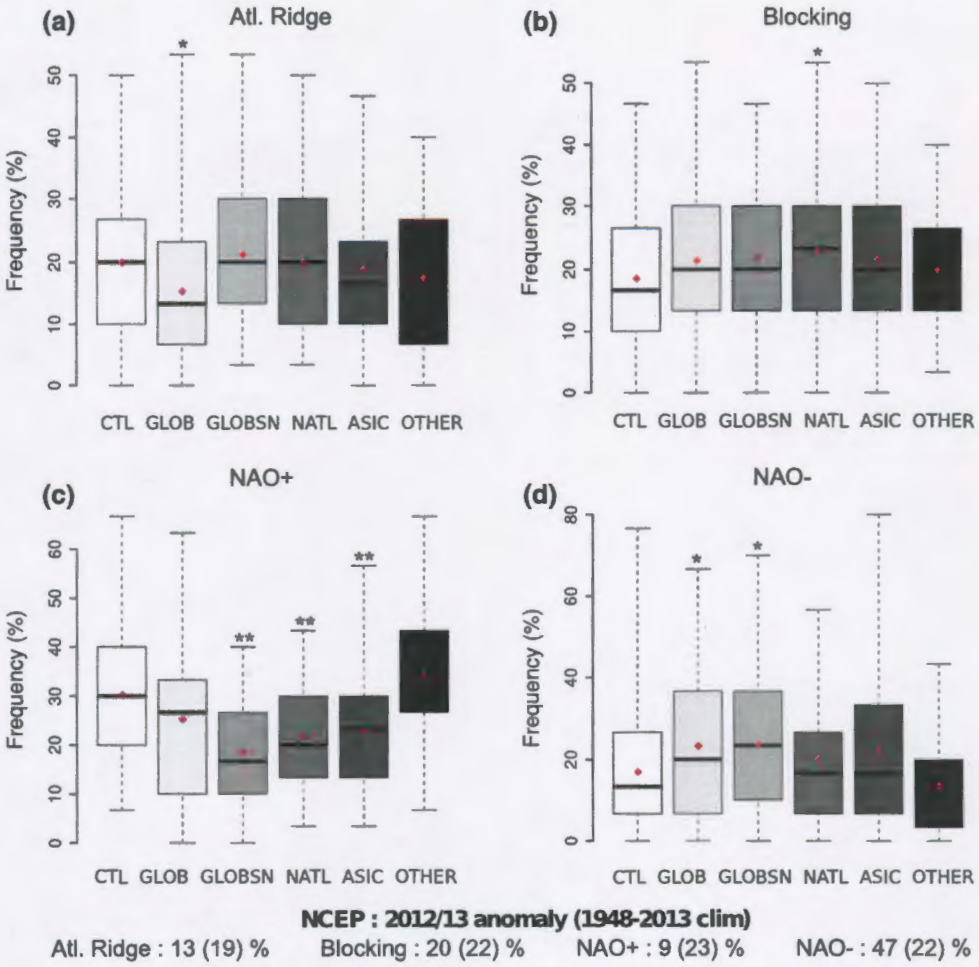

Fig. 4 Response of the North Atlantic intraseasonal weather regimes. Distribution of seasonal regime frequencies (50 years for each experiment) for each of the four weather regimes: **a** Atl. Ridge; **b** Blocking; **c** NAO+; **d** NAO−. *Boxplots* indicate the maximum, upper-quartile, median, lower-quartile and minimum of the distribution (*horizontal bars*). The mean of the distribution is shown by *red diamonds*, and *asterisks* indicate the significance level of the difference of the mean between the perturbation experiment and CTL: $*p < 0.1$; $**p < 0.05$ (Student *t* test). The frequencies of occurrence for the 2012–2013 winter in NCEP are indicated at the *bottom* (number in *parentheses* is the climatological value for 1948–2013)

Concerning the simulations, first of all it is important to note that the spread of the weather regime frequencies in CTL is comparable to the spread in the other experiments. This illustrates the importance of internal variability compared to the influence of imposed surface forcings. For example, atmospheric internal variability alone can generate some winters with a strong negative NAO (Fig. 4d, the maximum frequency for NAO− is almost 80 % in CTL). During some years, the impact of the surface forcings can therefore be completely overwhelmed by the atmospheric internal variability. Nevertheless, we observe a change in the probability distribution of the weather regimes. The most significant change is the decrease in the NAO+ regime, that is found in all experiments except OTHER. The largest decrease is found in GLOBSN since NATL, ASIC and the Siberian snow anomaly act together to reduce the likelihood of the NAO+ regime. The entire distribution is shifted towards lower values, especially in GLOBSN and NATL. The NAO response is not linear since only GLOB and GLOBSN show a significant change in the NAO− frequency, with a lower amplitude than for the NAO+ regime. The frequencies of the other two regimes are less disturbed, in agreement with observations. The combined mean anomaly of the negative and positive NAO regimes is 17 % in GLOBSN (Table 2). This supports the previous estimate based on the regression of SLP anomalies on the NAO pattern (Table 2) that the forced NAO response in our model represents about one third of the observed anomaly (17 % compared to 39 %).

3.2 Response in surface temperature

Figure 5 is similar to Fig. 2 but for the 2-m temperature. The observed temperature anomaly pattern is typical of the negative NAO (Fig. 5a) with lower than normal surface temperature over northern Eurasia and warmer than normal surface temperature over southern Eurasia and Greenland/eastern Canada (Hurrell and van Loon 1997). The cooling of northern Eurasia is not captured in GLOB (Fig. 5b), which is not surprising given the lack of high pressure anomaly over the Arctic in this experiment (Fig. 2b). This discrepancy is partly corrected when the Siberian snow is added (GLOBSN, Fig. 5c) due to the local thermodynamical cooling induced by increased snow mass over Siberia. The

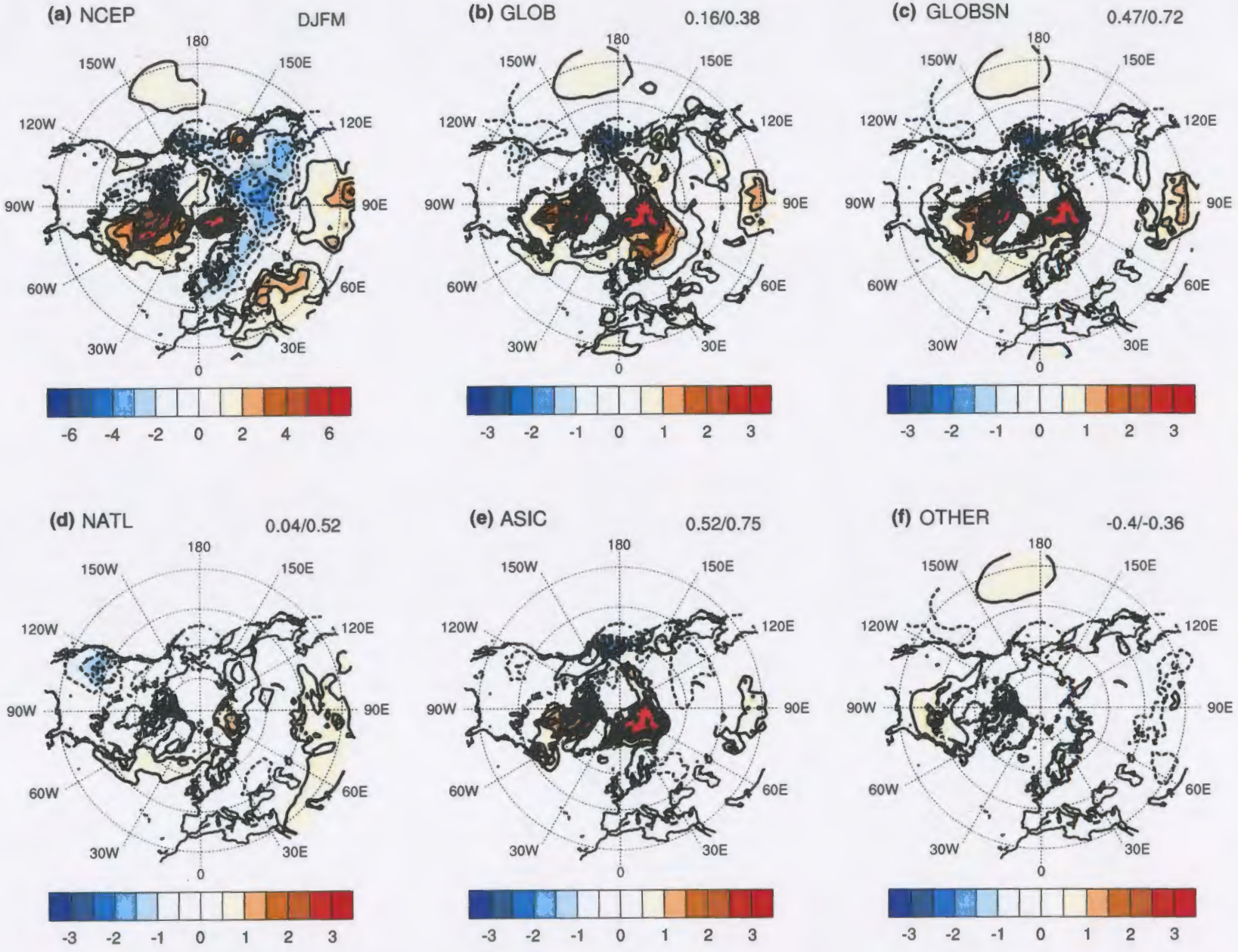

Fig. 5 Same as Fig. 2 except for the 2-m temperature (K)

agreement with NCEP is also slightly better over Europe, suggesting an additional response induced by higher pressure over Arctic and associated change in the atmospheric circulation. The response in NATL has low statistical significance except for negative anomalies in the western US. Once again, ASIC exhibits a very good pattern of the T2M anomalies (spatial correlations with NCEP of 0.52/0.75). This is of course expected over the Arctic ocean, where the absence/presence of sea ice strongly drives the surface temperature anomaly. A slight cooling of the mid-latitude continents is observed in ASIC (Fig. 2e) that supports the linkage between Arctic sea ice retreat and mid-latitude cooling (Honda et al. 2009; Petoukhov and Semenov 2010). However the amplitude of this response is small and has a low statistical significance. The thermal response of OTHER (Fig. 5f) is weak and opposite to observations, in line with the opposite dynamical response. Similar to the SLP field in Fig. 3a, Fig. 3b shows the impact of approximately removing the impact of OTHER from the T2M response of GLOBSN (subtracting OTHER from GLOBSN). This results in minor changes to the T2M field with only a small increase in the spatial correlation when OTHER is removed.

We now discuss the change in occurrence of extreme temperature. Figure 6 explores the response of cold extremes by computing the change in percentage of cold days (see Sect. 2c for details about the methodology) for both observations and the simulations. As illustrated in Fig. 6a, cold extreme days were more frequent than normal during the 2012–2013 winter over northern Europe and some regions of Asia. Interestingly, an increase of cold extremes is also found over the western US. As episodes of warm extreme temperature were also anomalously frequent during this winter (not shown), no significant anomaly of the mean temperature is found over the western US (Fig. 5a). Concerning the simulations, NATL induces an increase of cold days over western/central Europe and eastern US (Fig. 6d). This supports the notion that warm SST anomalies in the North Atlantic promote the occurrence of winter cold extremes over the adjacent continents through perturbation of the NAO regimes (Peings and Magnusdottir 2014b). The increase of cold extremes over the western US is also consistent with NCEP and with the significant response of the atmospheric circulation found in the North Pacific in NATL (Fig. 2d). GLOBSN shows a slight increase of cold extreme days over Siberia where the snow anomaly has been added, as well as over Europe since the negative NAO is promoted in this experiment. ASIC has a small impact, the main signal being a decrease in the frequency of cold extreme days in high latitudes. We end this discussion of the surface temperature responses by emphasizing that the pattern of cold extreme anomalies is more realistic when the influence of OTHER is removed (Fig. 3c), especially over Europe.

3.3 Tropics to extratropics teleconnections

In the following we investigate the possible causes for the dynamical responses identified in Sect. 3a. We first explore the role of tropical processes and associated large-scale teleconnections. Convection in the Intertropical Convergence Zone (ITCZ) is associated with precipitation and latent heat release in the free troposphere. This source of diabatic heating in the upper troposphere can induce some large-scale perturbations, such as enhancement of the ascending branch of the Hadley circulation and anomalous propagation of Rossby waves in the extratropics. The response in precipitation is shown in Fig. 7 along with the 850 hPa wind vectors. Precipitation increases in the tropical Atlantic, mostly in response to NATL (Fig. 7d). This response is mitigated by OTHER for which negative precipitation anomalies are found in the Atlantic (Fig. 7f) but is still exaggerated in GLOB and GLOBSN (Fig. 7b, c) compared to the observed anomaly. Over the tropical Pacific, a north-south dipolar anomaly is found that suggests a northward shift of the ITCZ. This is of course related to OTHER, but NATL also exhibits a similar pattern in the tropical Pacific, as well as the surface anticyclonic anomaly in the North Pacific (in line with the high pressure anomalies in this region, Fig. 2d).

Large-scale motions of the atmosphere that may have resulted from these tropical perturbations are investigated by using the stream function and velocity potential fields. Figure 8 shows the anomalies of the 200 hPa stream function and of the 200 hPa wind vectors. The stream function illustrates the rotational component of the atmospheric circulation and is thus useful for tracking the horizontal propagation of Rossby waves. Figure 9 shows the anomalies of the 200 hPa velocity potential and the divergent part of the 200 hPa wind. These non-rotational quantities illustrate the large-scale vertical motions of the atmosphere by identifying areas of convergence/divergence of the mass flow. NATL induces a Gill-Matsuno type response (Gill 1980) in the tropical Atlantic, with symmetric anticyclonic anomalies about the equator (Fig. 8d) associated with anomalous upper-level divergence in the tropical/North Atlantic sector (Fig. 9d). This response is consistent with the increase in precipitation in the tropical Atlantic (Fig. 7d) that is accompanied by an anomalous heating in the upper troposphere and a strengthening of the Atlantic Hadley circulation (see Fig. S2). This large-scale response in NATL is one of the main signatures of the overall response depicted in GLOB and GLOBSN (Fig. 9b–c). The divergent anomaly of the tropical Atlantic is associated with a wave train that tilts eastward over the North Atlantic and Arctic (Fig. 8b–d). The signal is equivalent barotropic in the North Atlantic where same-sign anomalies are found for the 850 hPa streamfunction anomalies in this region (Fig. S3). This

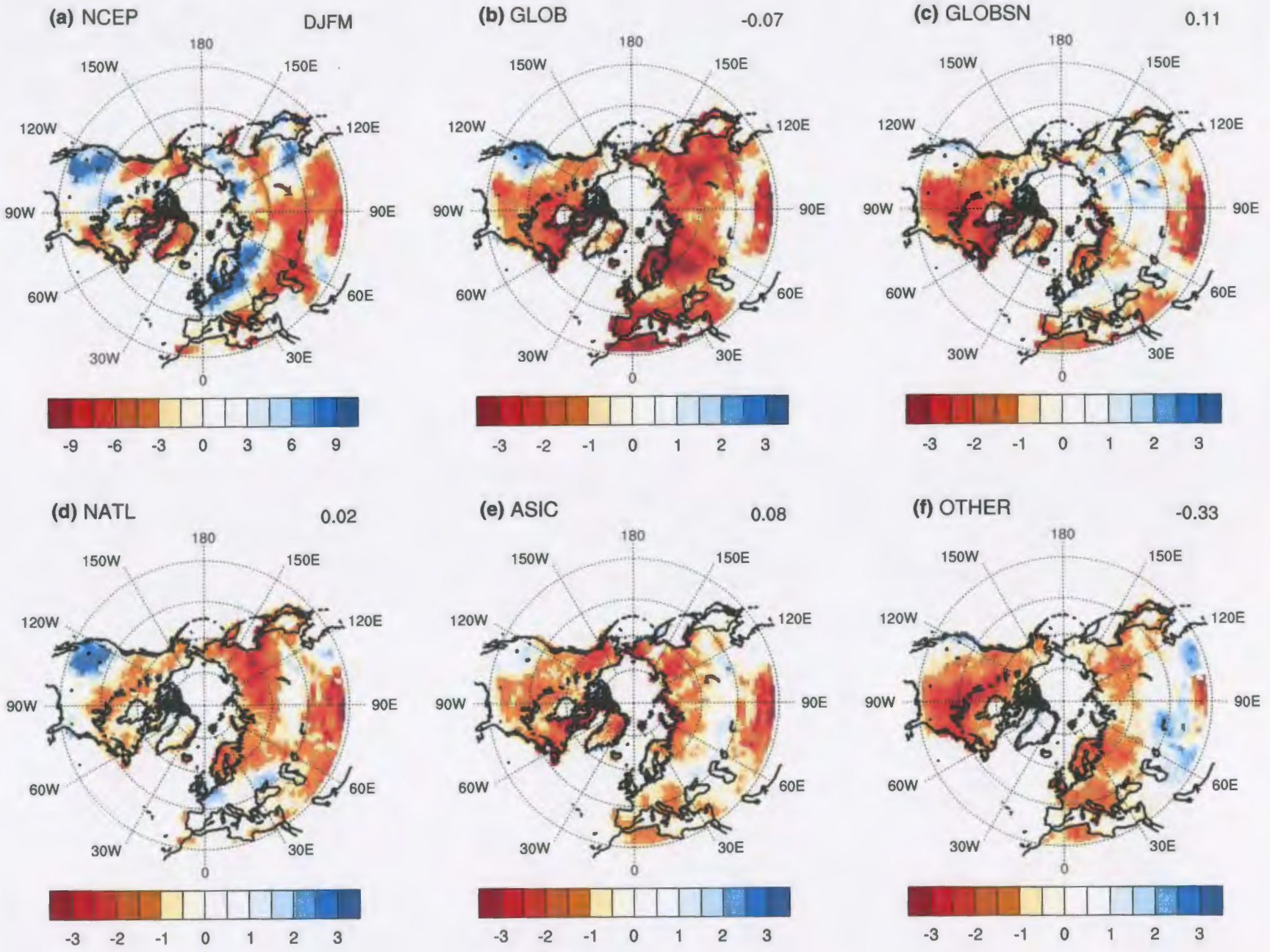
(a) NCEP
DJFM
(b) GLOB
-0.07
(c) GLOBSN
0.11
(d) NATL
0.02
(e) ASIC
0.08
(f) OTHER
-0.33
180
150W
150E
120W
120E
90W
90E
60W
60E
30W
30E
0
-9 -6 -3 0 3 6 9
-3 -2 -1 0 1 2 3

◀**Fig. 6** **a** Percentage of cold days (%, based on the 10th percentile of the daily distribution at each grid point) during the 2012–2013 winter. **b** Response in GLOB. The spatial correlation between the model response and the observed anomaly is indicated on the *top-right* of the plot. **c** Same as **b** for GLOBSN. **d** Same as b for NATL. **e** Same as **b** for ASIC. **f** Same as **b** for OTHER

response is a frequently encountered pattern that is associated with the negative NAO in response to tropical Atlantic SST anomalies (Okumura et al. 2001; Drevillon et al. 2003; Peng et al. 2005; Losada et al. 2008) and has also been identified as a reflected wave train again associated with the negative NAO (Abatzoglou and Magnusdottir 2006). As in the quoted studies, the North Atlantic response in our experiments is reinforced by the transient-eddy feedback of the mid-latitudes (see next section).

The enhancement of the Hadley cell in the Atlantic is an important signal of our simulations but it was not detected during the winter 2012–2013. Indeed, there is no divergence anomaly or reinforcement of the subtropical branch of the Hadley cell in the tropical Atlantic in NCEP (Fig. 9a and Fig. S2). The cause for the overestimate of the response in the tropical Atlantic is unclear and is beyond the scope of this study. It is plausible that the absence of ocean/atmosphere feedbacks in the model is responsible since it results in an exaggerated increase of deep convection and precipitation where warm SST anomalies are prescribed in the tropics (Kitoh and Arakawa 1999). On the other hand, the wind-evaporation-SST mechanism results in a positive feedback in the tropical Atlantic (Xie and Carton 2004), such that the ocean-atmosphere coupling might actually result in an increase of the overestimate by reinforcing the warm SST anomaly north of the equator. It is also possible that the increase in convection and the signature of the Atlantic wave train are overshadowed by other processes in NCEP for the 2012–2013 winter.

In the Pacific, a significant signal is found in OTHER in which a wave train extends from the tropical Pacific to the eastern Arctic (Fig. 8f). This teleconnection favors the anomalous Pacific high and the northward shift of the North Pacific jet stream identified previously. A somewhat similar wave train can be seen in NCEP (Fig. 8a) except the cyclonic anomalies in the eastern Arctic are not present in NCEP. As a result, low surface pressure anomalies are found in OTHER in this region (Fig. 2f) while high pressure anomalies were observed (Fig. 2a). This teleconnection between the tropical Pacific and the Arctic that has the wrong sign provides a partial explanation for the opposite signed response of the NAO/NAM in OTHER.

3.4 Response of the mid-latitude baroclinic activity

Figure 10a shows the observed anomaly of the zonal wind at 200 hPa, around the altitude of the jet stream. In line with the negative phase of the NAO, a southward shift of the jet stream is found in the North Atlantic. During the 2012–2013 winter, the reduced polar jet stream in the northern part of the basin has favored the intrusion of polar air over northern Europe and eastern North America, resulting in frequent occurrences of cold extreme events. An opposite anomaly of the westerly flow is visible in the North Pacific, where the polar jet stream is shifted northward. The zonal wind anomalies of the North Atlantic sector are remarkably well captured by our simulations (Fig. 10b–e, with model climatology in red contours in b) except for OTHER which promotes the positive phase of the NAO and thus has an opposite shift of the North Atlantic zonal wind (Fig. 10f). The North Atlantic signal is well captured in NATL (Fig. 10d) with the southward displaced polar jet and strengthened subtropical jet. The response is also in the same sense for ASIC (Fig. 10e) and for the Siberian snow anomaly (GLOBSN vs GLOB, Fig. 10b, c) such that the larger response is found in GLOBSN. The amplitude of the response in the North Atlantic represents about 30 % of the observed anomalies, in line with the amplitude of the NAO response (Sect. 3a). The northward shift of the North Pacific jet stream is also captured by our model. OTHER has the greatest contribution to that response through the Rossby wave train that originates in the tropical Pacific (Fig. 8f), but NATL and to a lesser degree ASIC also show this response.

The zonal mean flow modification is associated with a southward shift of the eddy transient activity over the North Atlantic basin (Fig. 11a, see Sect. 2c for definition of the eddy transient activity). The change in the course of the storm track is captured in GLOB and GLOBSN (Fig. 11b–c), but not as well as the anomaly of the zonal wind (lower agreement over the North Atlantic compared to Fig. 10). NATL is the main driver of the increase of transient activity around 40°N (Fig. 11d), while ASIC slightly decreases the transient activity in the northern part of the basin and over northern Europe (Fig. 11e). The change in transient activity is partly a response to the zonal mean flow modification induced by the tropical Atlantic forcing, but is also a mechanism for explaining the extratropical response. Previous GCM experiments have shown that the strengthening of the subtropical jet modifies the baroclinicity and the eddy transient activity, that in turn interacts with the low-frequency anomalous circulation and reinforces the westerly flow anomalies (Drevillon et al. 2003; Peng et al. 2005; Losada et al. 2008). The feedback of the transient eddy activity on the zonal mean flow anomaly can be estimated using the E-vector of Hoskins et al. (1983). Figure 12 shows the E-vector anomalies and their divergence (shading) at 200 hPa (see Sect. 2c for definition of the E-vector). In observations, the anomalous eddy transient activity induced an easterly forcing on the mean flow in the northeast of the

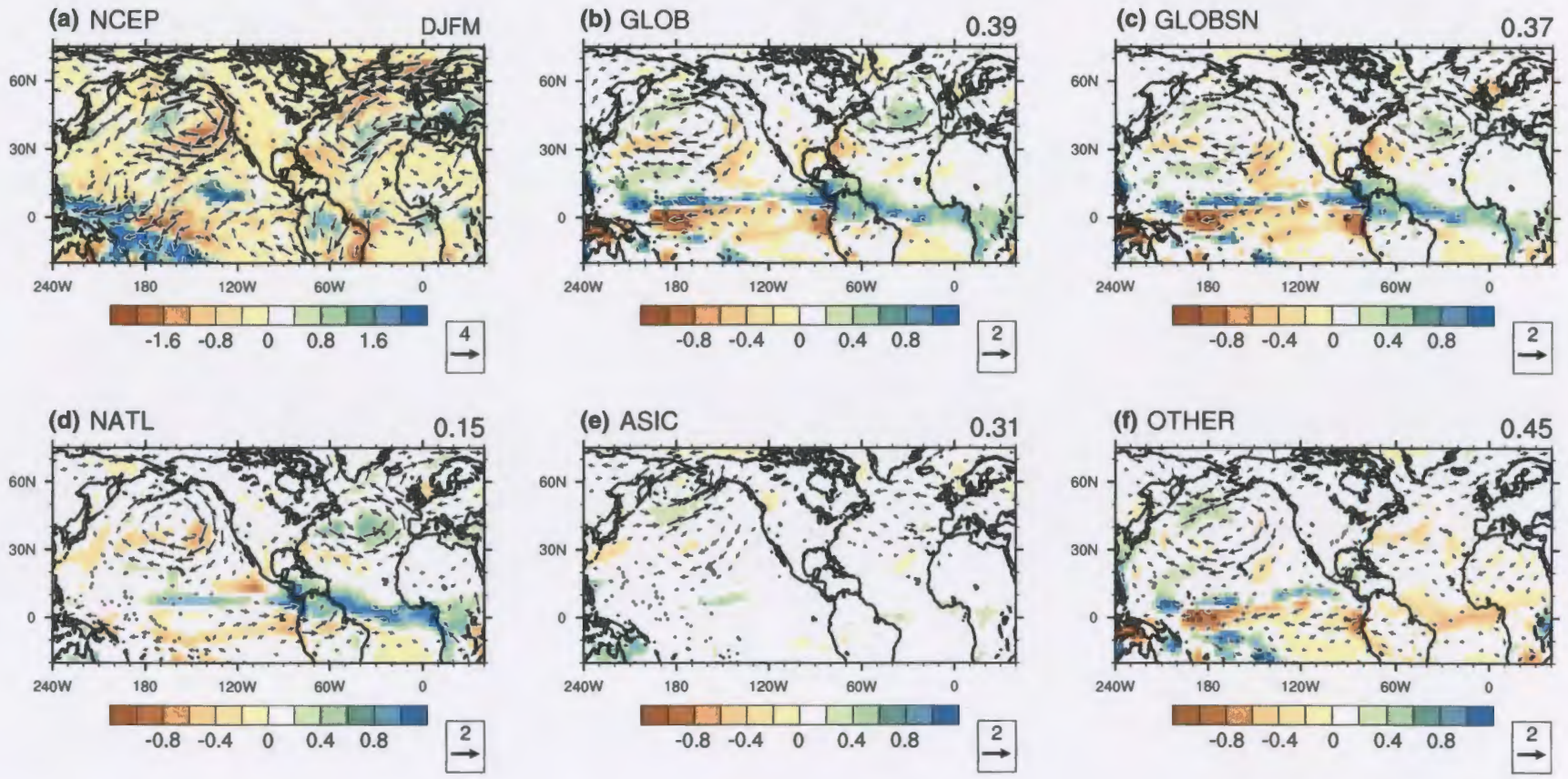

Fig. 7 Same as Fig. 2 except for precipitation (mm day^{-1}, *shading*) and the 850 hPa wind vectors (m s^{-1}). Only precipitation response that is significant at the 95 % confidence level is shown. The spatial correlation between the model response and the observed anomaly of precipitation is indicated on the *top-right* of the plot

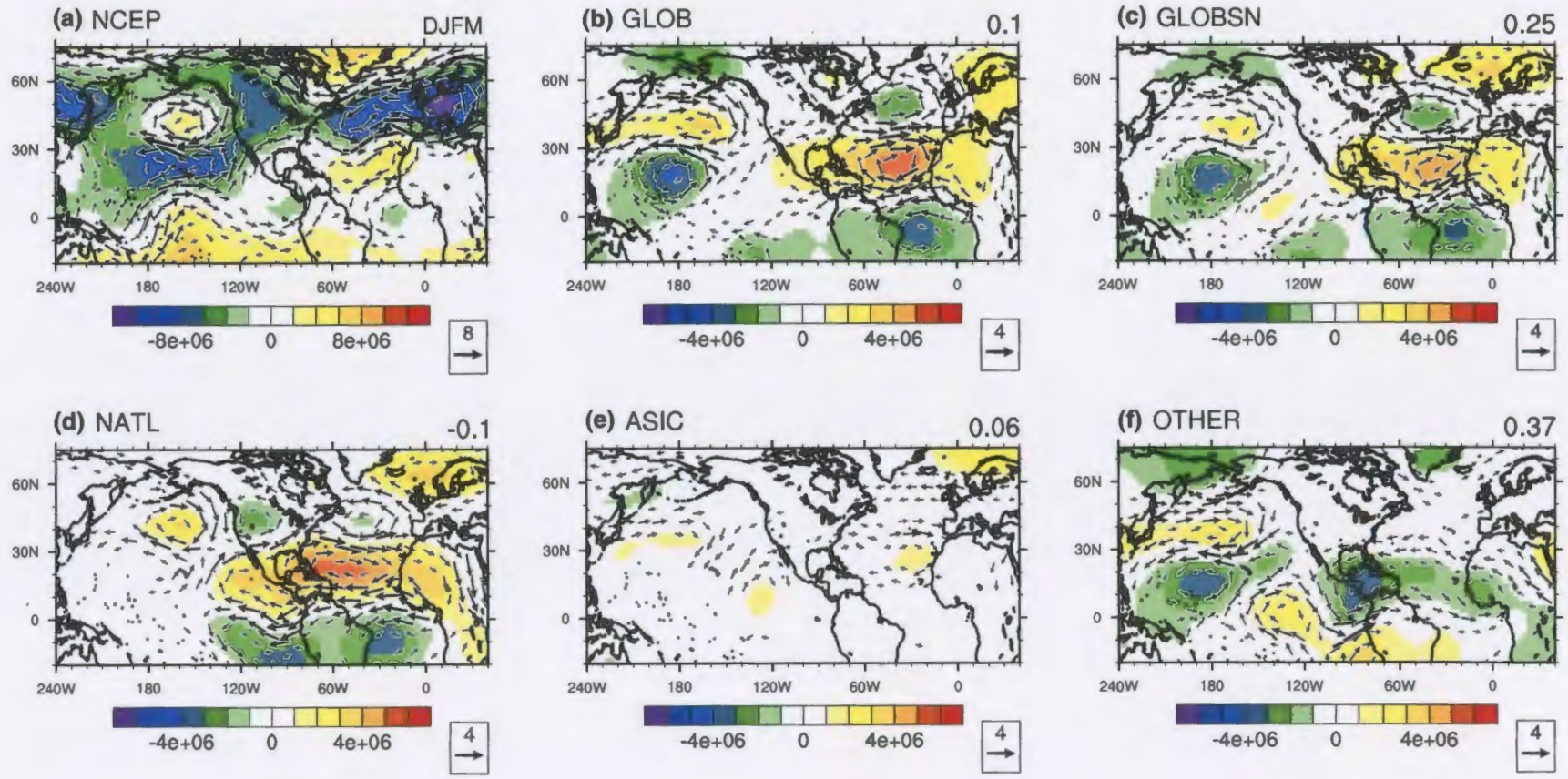

Fig. 8 Same as Fig. 2 except for the 200 hPa streamfunction (kg s^{-1}, shading) and the 200 hPa wind vectors (m s^{-1}). Only the streamfunction response that is significant at the 95% confidence level is shown. The spatial correlation between the model response and the observed anomaly of streamfunction is indicated on the *top-right* of the plot

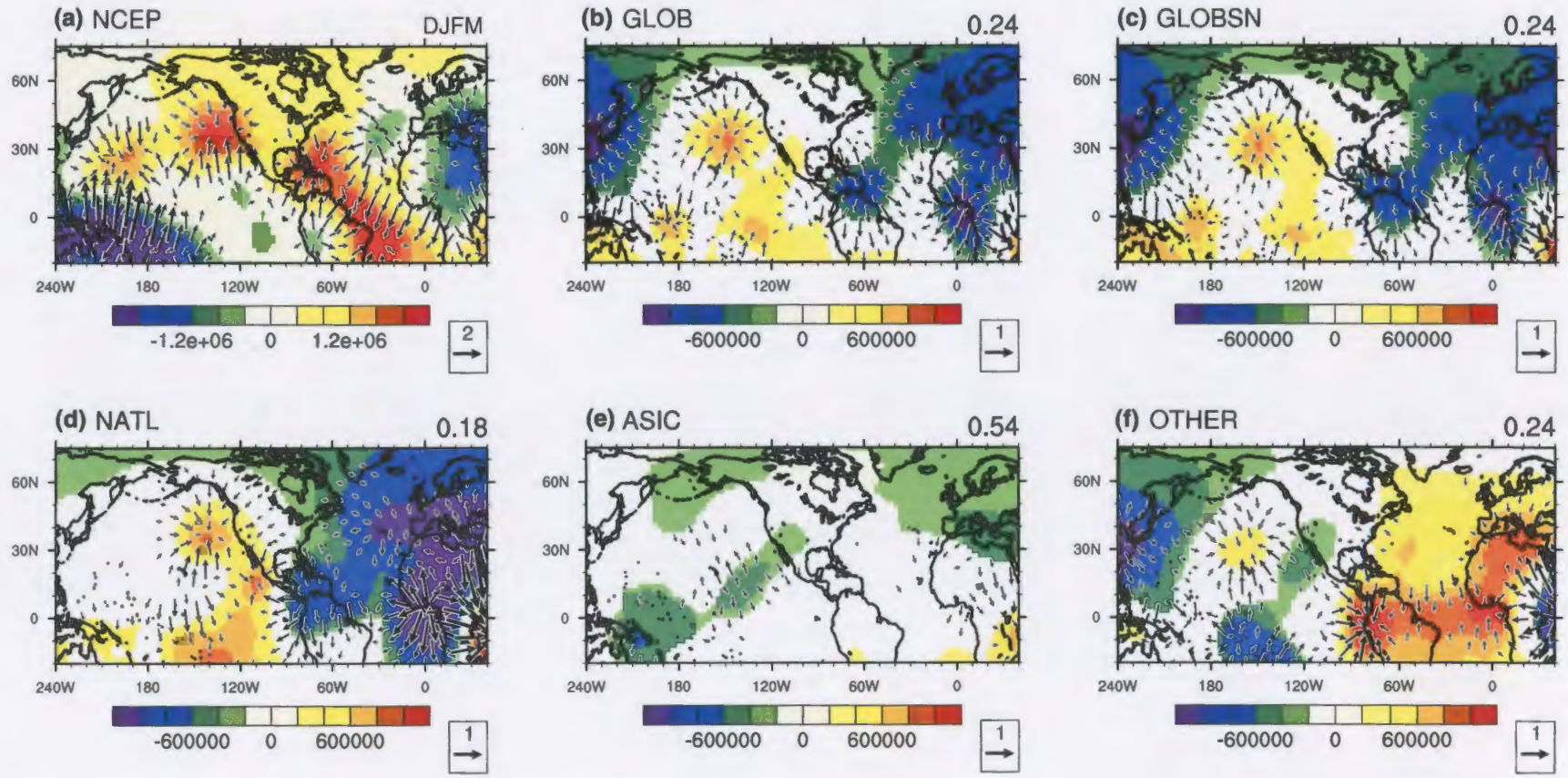

Fig. 9 Same as Fig. 2 except for the 200 hPa velocity potential ($m^2\ s^{-1}$, shading) and the 200 hPa divergent wind ($m\ s^{-1}$). Only the velocity potential response that is significant at the 95 % confidence level is shown. The spatial correlation between the model response and the observed anomaly of velocity potential is indicated on the top-right of the plot

basin (convergence of the E-vector, Fig. 12a) that helped to maintain the negative anomalies of the westerly wind in this region. Southward, the opposite is found with a preponderance of E-vector divergence and an acceleration of the westerly flow. Note that the divergence field is noisy due to the fact that it is computed from synoptic small-scale fields. The model simulates the eddy-mean flow interactions quite realistically, with a corresponding pattern of E-vectors and an eddy-driven acceleration (deceleration) of the zonal mean flow in the southern (northern) part of the North Atlantic basin (Fig. 12b–c). NATL contributes to the eddy-driven acceleration around 40°N (Fig. 12d), with also a contribution by ASIC in the east Atlantic (Fig. 12e) and by the Siberian snow anomalies in the western Atlantic (GLOBSN vs GLOB, Fig. 12b–c). A similar picture is found over the North Pacific, where eddy activity anomalies reinforce the zonal wind anomalies (not shown). In line with previous work, the eddy-mean flow feedback is therefore an amplification mechanism for the large-scale atmospheric circulation response to tropical forcing in our experiments.

Although the feedback of the baroclinic eddies is an amplifying mechanism of the mid-latitude response, the influence of extratropical Atlantic SST remains unclear. It is well-known that tropical SST anomalies produce a stronger atmospheric response compared to extratropical SST anomalies. Numerous papers (e.g., Kushnir et al. 2002) have shown that extratropical SST anomalies have a small influence compared to internal variability of the atmosphere. Consequently, one question is whether the signal that we identify in NATL is only induced by the tropical part of SST forcing. We did not perform specific experiments to fully answer this question in the present case study but we have some insight on this issue. We have performed numerical experiments that explore the role of subtropical vs mid-latitude Atlantic SST anomalies (these results will be part of a forthcoming study). In these simulations also performed with CAM5, both the tropical and extratropical part of the SST forcing in the Atlantic are needed to obtain a significant response in the NAO and the jet stream. The response is weak with little significance when only one part of the forcing is imposed in the model. It becomes comparable to the response described in the present study when both parts of the SST forcing are included. Even so these simulations are not directly comparable with the present study since they are not specific to the 2012–2013 winter, they demonstrate that extratropical North Atlantic SST anomalies play an active role and reinforce the atmospheric response to tropical SST anomalies. In particular, SST anomalies in the Gulf stream region have the potential to significantly impact the transient activity through heat flux reponse and associated modification of the baroclinicity, as stated in recent studies (Gulev et al. 2013; Peings and Magnusdottir 2014b).

3.5 Response in the polar stratosphere

Another possible extratropical mechanism that may explain the atmospheric anomalies identified in this study involves the perturbation of the stratospheric polar vortex. The stratospheric polar vortex is an important source of variability of the NH winter climate that can significantly impact surface parameters. Indeed, stratospheric perturbations can propagate toward the surface through complex troposphere-stratosphere interactions (Waugh and Polvani 2010). Figure 13 shows the response in zonal wind at the 10 hPa level. This field allows us to examine how the stratospheric polar vortex responds in our experiments. The polar vortex was anomalously warm during the 2012–2013 winter, as illustrated by low stratospheric westerlies around the North Pole (Fig. 13a). Even though the model does not simulate such a strong signal, the pattern of the response matches the anomaly in observations (0.76/0.88 spatial correlations in GLOBSN, Fig. 13c). NATL, ASIC and the Siberian snow anomalies act together to reduce the stratospheric polar vortex. NATL has a stronger impact over the North Atlantic portion of the jet (Fig. 13d) while ASIC exhibits some significant anomalies above the Kara-Barents sea (Fig. 13e). The Siberian snow anomaly also reinforces the weakening of the polar vortex (GLOBSN vs GLOB, Fig. 13b–c).

The seasonal response depicted in Fig. 13 masks a strong intraseasonal variability. The 2012–2013 winter was characterized by the occurrence of a sudden stratospheric warming of the stratosphere in mid-winter, which is a phenomenon typically associated with negative values of the tropospheric NAM/NAO some weeks later due to the timing of downward propagation of stratospheric anomalies (Baldwin and Dunkerton 2001). The mid-winter SSW was thus an important feature of the atmospheric circulation that may have been forced by the surface forcings. Figure 14 shows the daily evolution of the vertical distribution of horizontally averaged geopotential response/anomaly over the polar cap (north of 65°N). This diagnostic is a good proxy for the daily evolution of the NAM index as a function of altitude (Baldwin and Thompson 2009), a positive (negative) anomaly being associated with a negative (positive) value of the NAM index. In observations, the warming of the polar vortex is clearly visible (Fig. 14a) starting in early January and lasting until mid-February. All experiments tend to reproduce a weakening of the polar vortex in mid-winter, but the response is small with low statistical significance (Fig. 14b–f). The signal is strongest in GLOBSN (Fig. 14c), in line with Siberian snow anomalies perturbing the stratospheric polar vortex (Fletcher et al. 2009; Peings et al. 2012). ASIC induces a late-winter weakening of the

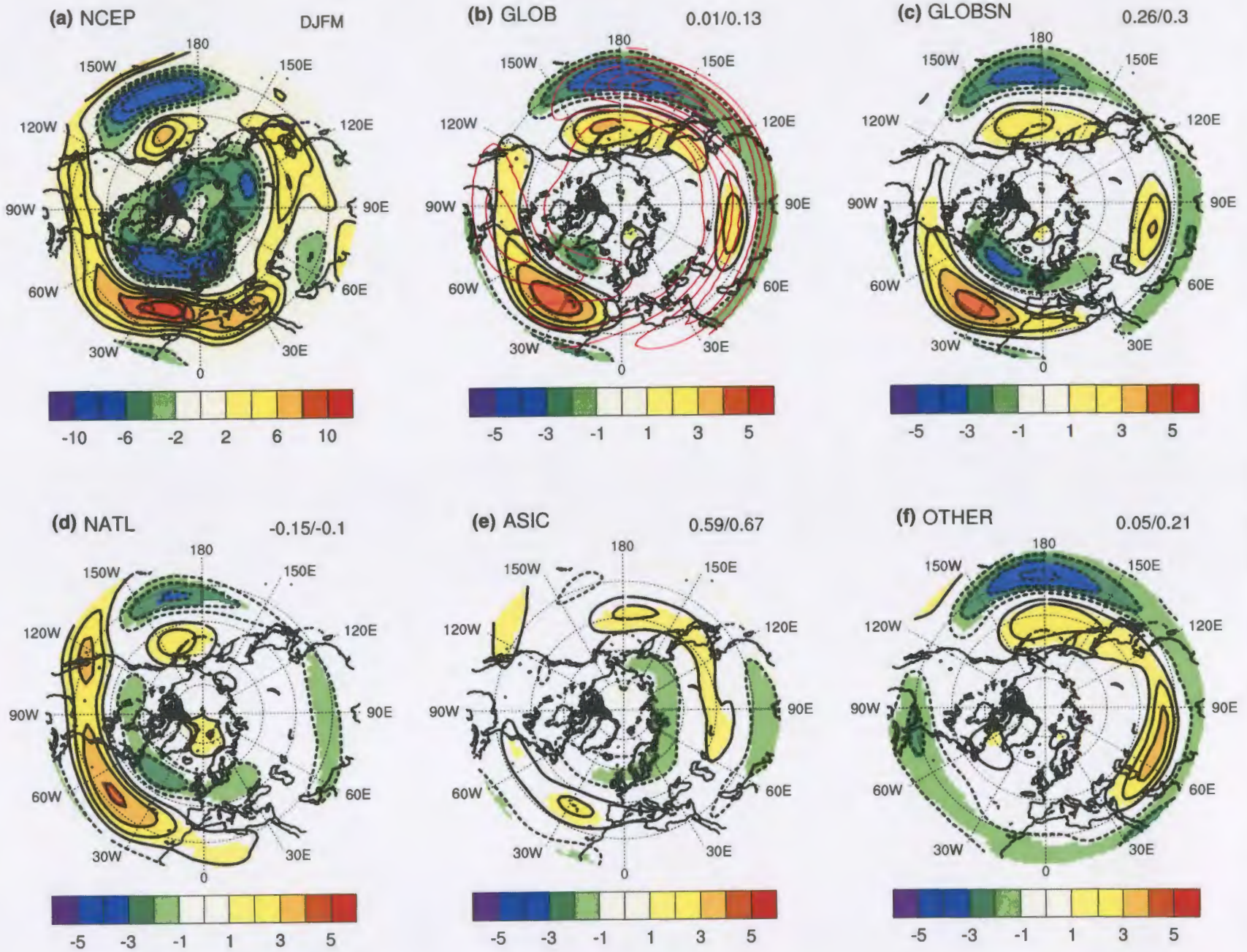
(a) NCEP
DJFM
(b) GLOB
0.01/0.13
(c) GLOBSN
0.26/0.3
(d) NATL
-0.15/-0.1
(e) ASIC
0.59/0.67
(f) OTHER
0.05/0.21
180
150W
150E
120W
120E
90W
90E
60W
60E
30W
30E
0
-10 -6 -2 2 6 10
-5 -3 -1 1 3 5

◀**Fig. 10** Same as Fig. 2 except for the 200 hPa zonal wind (m s^{-1}). The climatology computed from CTL is superimposed in red contours (interval of 10 m s^{-1} between 20 and 70 m s^{-1}) in **b**

polar vortex (Fig. 14e) consistent with Peings and Magnusdottir (2014a).

The slight slowdown of the polar westerly winds is associated with an enhanced upward propagation of stationary waves from the troposphere into the stratosphere (see Fig. S4, anomalies of EP-flux and zonal mean zonal wind). The upward EP-flux anomaly is especially noticeable in GLOBSN (Fig. S4c, effect of Siberian snow) and in ASIC where the negative zonal mean zonal wind anomaly in high latitudes is significant at the 90 % confidence level all along the vertical (Fig. S4e). This interesting signal confirms the potential of recent Arctic sea ice anomalies for inducing significant NAM anomalies that propagate downward through stratosphere-troposphere coupling (Peings and Magnusdottir 2014a).

When looking at the stratospheric response, we have to keep in mind that this study uses a low-top model. Omrani et al. (2014) pointed out the importance of the stratospheric representation in the response to AMO SST anomalies. They found a significant warming of the polar stratosphere only in their simulations performed with a high-top model. Despite its low-level lid (around 3 hPa), our model is able to simulate SSWs (defined as a reversal of the climatological westerly winds at 10 hPa and 60°N). It is therefore quite relevant to discuss the stratospheric response in our simulations. However, the weak response of the polar vortex that we obtain is possibly related to the shortcomings of our model concerning the representation of the stratosphere.

4 Conclusion

The 2012–2013 winter was characterized by an anomalous persistence of the negative phase of the NAO/NAM (NAO index of −1.66 when the EOF-based index is used). The North Atlantic jet stream and the storm track were shifted southward, and a significant stratospheric warming event developed at the beginning of January 2013. Altogether, these dynamical anomalies resulted in colder than normal conditions and episodes of frigid weather over Eurasia. At the same time, opposite conditions were observed in the North Pacific where high pressure anomalies prevailed, resulting in a northward shift of the jet stream.

Perturbation experiments performed with CAM5 suggest that part of the large-scale anomalies observed during this winter were driven by surface conditions, the rest being related to internal variability of the atmosphere or other undetermined external forcings. The study focused on the specific role of low sea ice concentration in Arctic, excess of snow over Siberia and warmer than normal SST in the North Atlantic (associated with the current positive AMO polarity). These surface parameters exhibited significant anomalies during the 2012–2013 fall/winter, which makes this season an interesting case study for exploring their role on the wintertime NH atmospheric circulation. According to our ensemble simulations, each of the three climatic anomalies tend to promote the observed negative NAO of the 2012–2013 winter. Altogether, the combined response of the NAO to the three surface forcings accounts for about 30 % of the observed NAO anomaly. However, the response of the NH atmospheric circulation and the associated physical mechanism differ significantly from one surface forcing to the other.

The tropical/North Atlantic SST anomalies have a greater influence on the southern lobe of the NAO than on the northern lobe (significant negative pressure anomalies in the North Atlantic but no positive anomaly in high latitudes). A large part of the atmospheric response arises from the tropical Atlantic SST anomalies that strengthen the upward branch of the Hadley cell near the equator. The upper-level divergent flow induces a Rossby wave train towards the extratropics and a southward shift of the mid-latitude jet stream. In line with the eddy-mean flow interaction theory, the change in eddy transient activity reinforces the zonal flow anomalies and helps to maintain the negative NAO signal. This mechanism is supported in previous findings (Drevillon et al. 2003; Peng et al. 2005; Losada et al. 2008) but was not identified during the 2012–2013 winter. In consequence, one part of the good agreement between simulations and observations concerning the NAO signal arises from an exaggerated response in the tropical Atlantic. In comparison, the north Atlantic SST anomalies have a smaller impact even though additional experiments (not discussed in the present study) suggest that both tropical and extratropical SST anomalies are needed to obtain a significant response of the extratropical atmospheric circulation in CAM5.

The response to a decrease of Arctic sea ice is low but it is realistic in terms of the spatial pattern of the anomalies for SLP, upper-level zonal wind and surface temperature response. In line with Peings and Magnusdottir (2014b), the Arctic SIC anomalies force an increase in upward stationary waves into the stratosphere that causes a late-winter weakening of the polar vortex and negative NAM anomalies in the entire atmospheric column. According to our results, the recent Arctic sea ice decline therefore contributes to the recent trend towards the negative NAO/NAM in late winter, but with only modest amplitude compared to the atmospheric variability. Cohen et al. (2012) argued that the negative trend of the NAO/NAM is related to Arctic sea ice loss through a Siberian snow pathway. They suggest that the sea

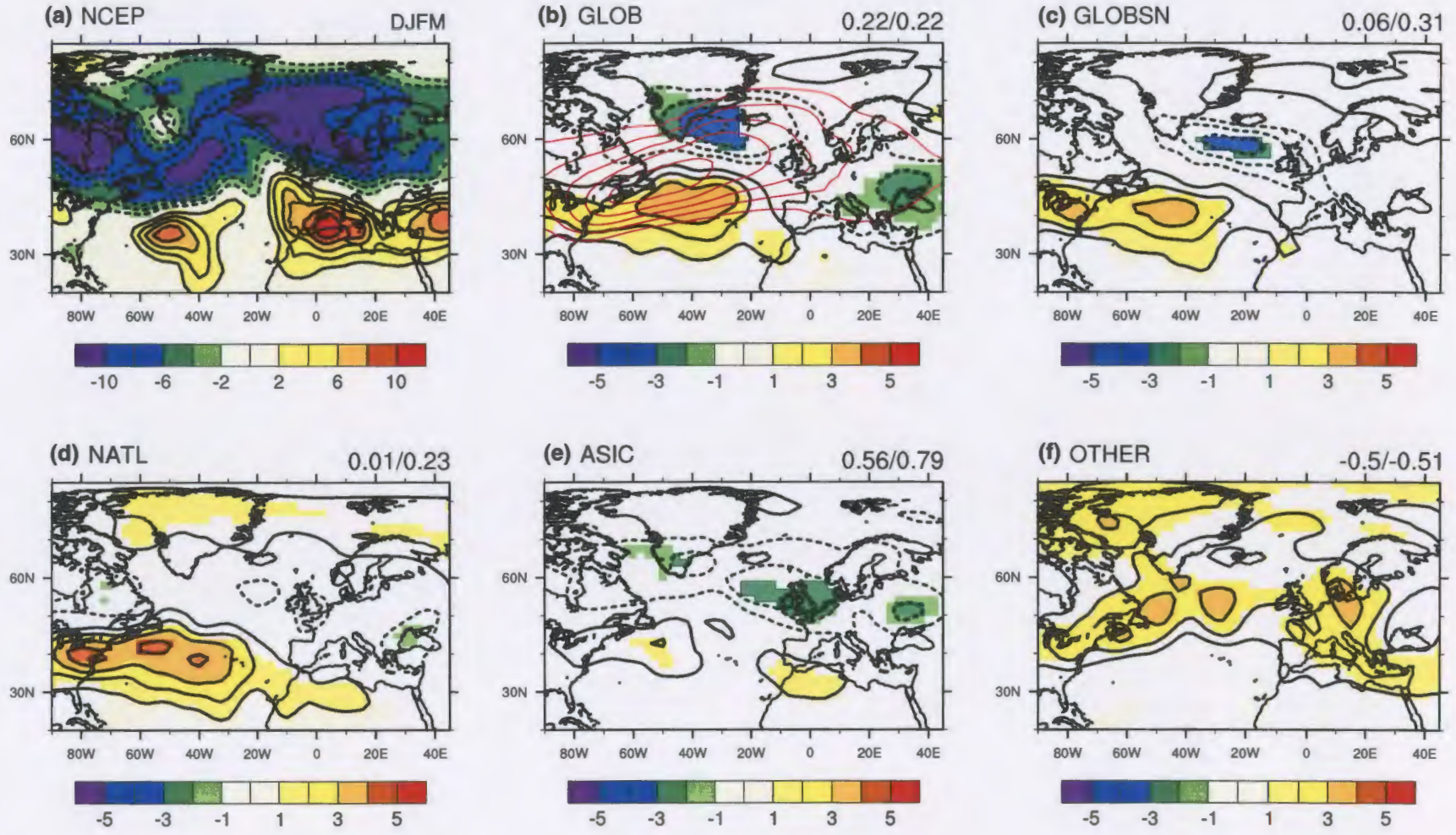

Fig. 11 Same as Fig. 2 except for the eddy transient activity (m) over the North Atlantic. The climatology computed from CTL is superimposed in red contours (interval of 6 m between 30 and 60 m) in b

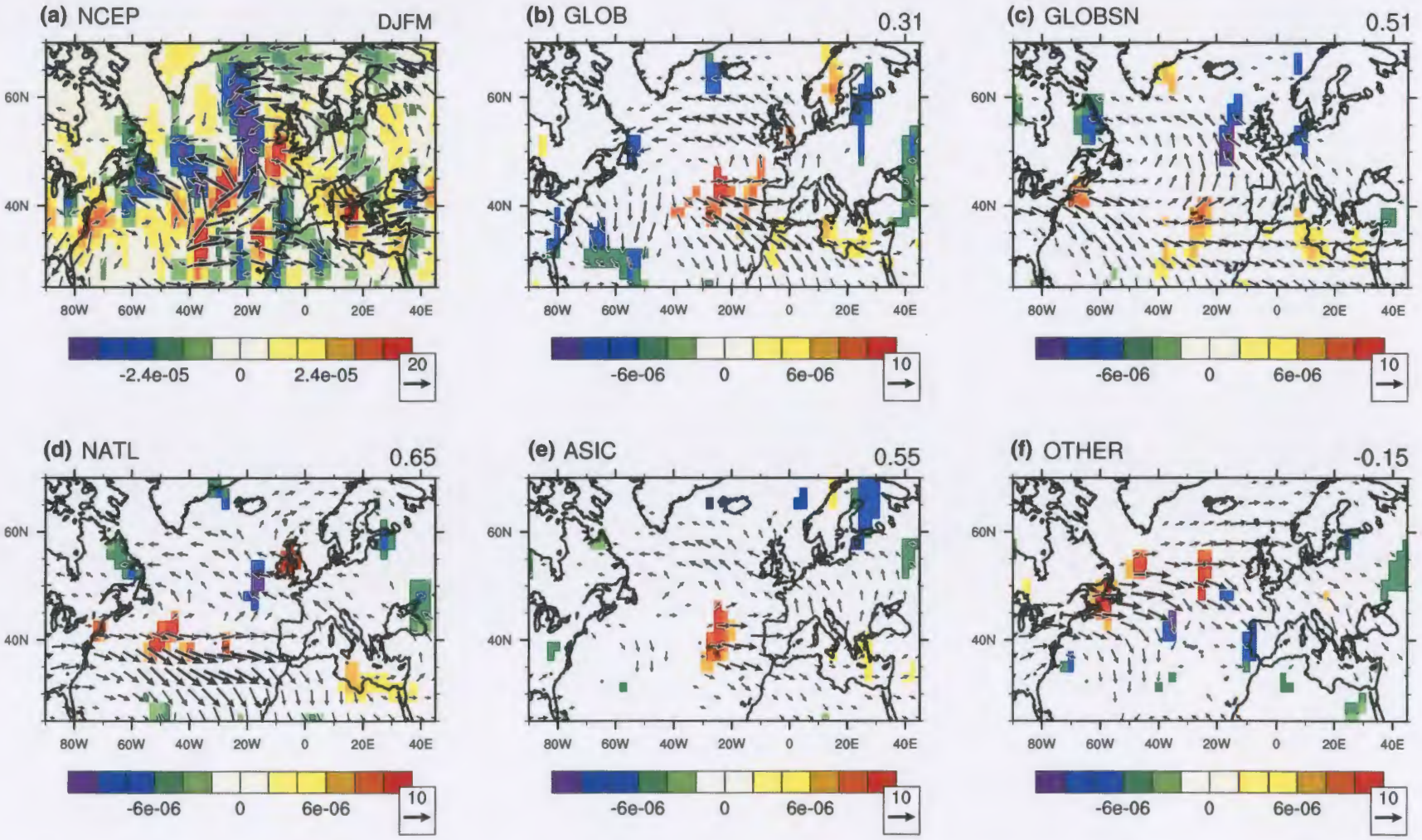

Fig. 12 Same as Fig. 2 except for the divergence of E-vector (m s^{-2}, shading) and the 200 hPa E-vectors (m^2 s^{-2}). Only the divergence response that is significant at the 95 % confidence level is shown. The spatial correlation between the model response and the observed anomaly of divergence is indicated on the *top-right* of the plot

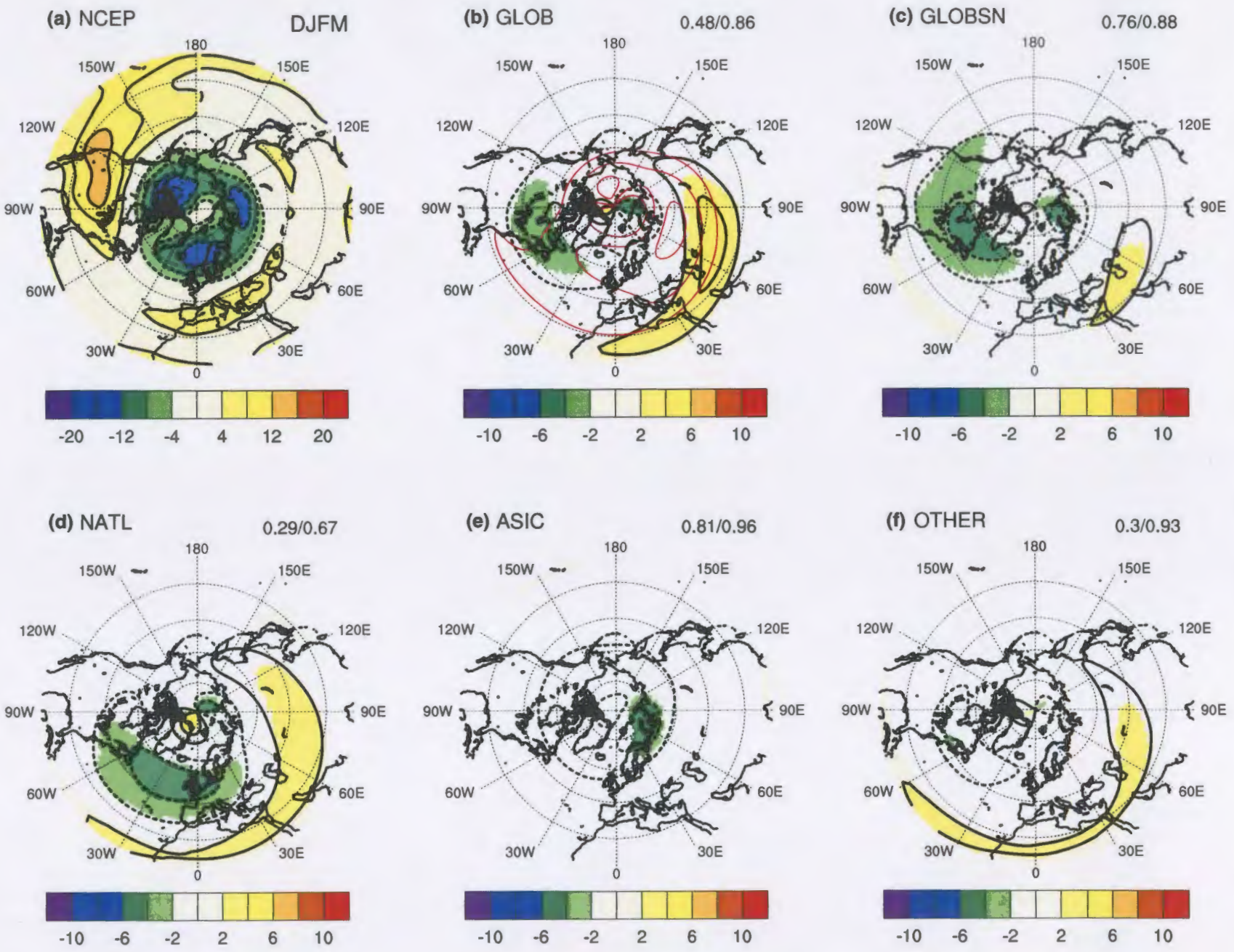
(a) NCEP
DJFM
(b) GLOB
0.48/0.86
(c) GLOBSN
0.76/0.88
(d) NATL
0.29/0.67
(e) ASIC
0.81/0.96
(f) OTHER
0.3/0.93
180
150W
150E
120W
120E
90W
90E
60W
60E
30W
30E
0
-20 -12 -4 4 12 20
-10 -6 -2 2 6 10

◀**Fig. 13** Same as Fig. 2 except for the 10 hPa zonal wind (m s^{-1}). The climatology computed from CTL is superimposed in red contours (interval of 10 m s^{-1} between 20 and 70 m s^{-1}) in **b**

ice melt increases evaporation and precipitation in high-latitudes, inducing an increase in snow cover that promote the negative NAO/NAM through land-atmosphere interactions. Our study illustrates that in addition to this indirect effect, high-latitude sea ice anomalies can promote a small NAO/NAM response by themselves. Indeed, the indirect effect of sea ice through snow is not at work in ASIC since no significant snow anomaly is found over Siberia (not shown). Nevertheless, our idealized experiment with a positive Siberian snow anomaly confirm the remote influence of snow. The increase of pressure in the Arctic is consistent with previous snow-atmosphere interaction studies, though the stratosphere-troposphere coupling is low in the present study.

The response of the other SST/SIC anomalies (i.e. Pacific, Indian and South Atlantic oceans) is opposite (positive NAO/NAM) and thus overshadows the negative NAO pattern induced by the three other forcings when all forcings are included. When removing the influence of OTHER by simply subtracting GLOBSN and OTHER (assuming a linear response to the forcings), the combined response of the NAO is two times larger and represents about 65 % of the observed anomaly (Table 2). The response to OTHER is possibly too strong in our model due to an exaggerated influence of tropical forcing in the NH extratropics, but further simulations would be necessary to fully investigate this question. In any case, the opposite response of the OTHER simulation suggests that the NH atmospheric anomaly of the 2012–2013 winter was unrelated to a tropical Pacific or Indian ocean signal. At least for the 2012–2013 winter, this result is in disagreement with a recent study that attributes

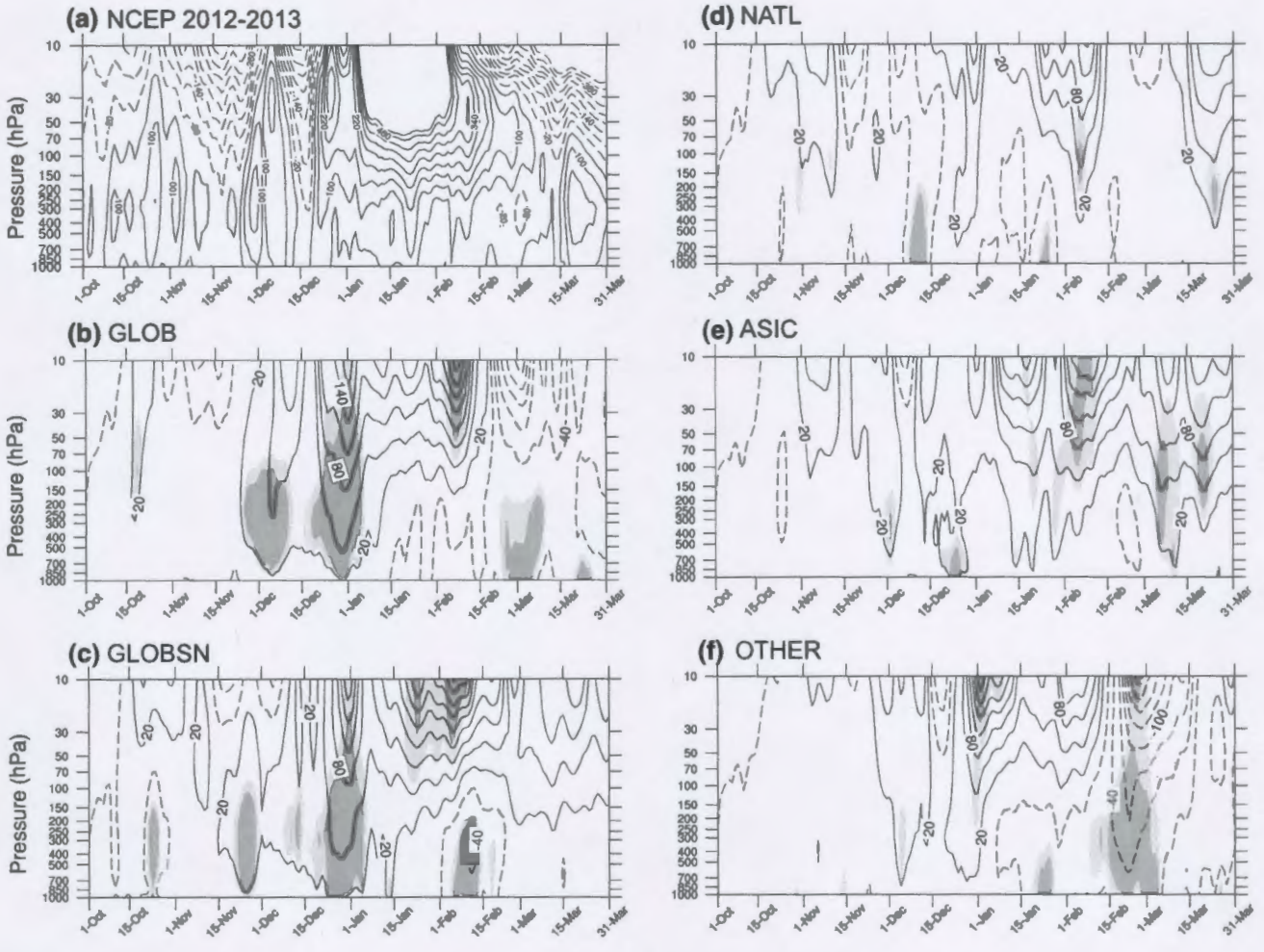

Fig. 14 Time–pressure cross section of the daily polar cap anomaly/response (m, geopotential averaged north of 65°N) for: **a** NCEP; **b** GLOB; **c** GLOBSN; **d** NATL; **e** ASIC; **f** OTHER. *Light* (*dark*) *shading* indicates significance at the 90 % (95 %) significance level. The *contour* interval is 30 m

the recent negative trend of the NAO and cold winters in Europe to quasi-stationary Rossby waves that originate from the tropical Pacific (Trenberth et al. 2014).

The response to our experiments and the mechanisms suggested are mostly consistent with various previous studies. This case study illustrates that the forced component of the NAO is not negligible compared to the atmospheric internal variability, especially when several boundary forcings act in the same direction. Of course, the different responses identified in our experiments represent an upper bound of predictability since the surface forcings were known and imposed to the model through winter. Nevertheless, improvements in the representation of these boundary forcings and of their associated large-scale teleconnections in the coupled ocean-atmosphere models would benefit dynamical seasonal forecasting. Compared to these models, our AGCM does not account for some important processes of the climate system, the influence of which will have to be quantified. In particular, the non-interactive ocean is a strong limitation. The use of a slab-ocean model would partially resolve the shortcoming, but how to prescribe observed SST anomalies in such a model is challenging. Also, numerical experiments with a better-resolved stratosphere using a high-top model would help to assess the importance of stratospheric processes. Despite these limitations, we believe that the present study clarifies the role of each potential mechanism in forcing the observed NH climatic anomalies of the 2012–2013 winter.

Acknowledgments We thank two anonymous reviewers for comments on the manuscript. This work was supported by NSF Grant AGS-1206120. High-performance computing was performed at NCAR's CISL.

References

Abatzoglou JT, Magnusdottir G (2006) Opposing effects of reflective and non-reflective planetary wave breaking on the NAO. J Atmos Sci 63:3448–3457

Adler RF, Huffman GJ, Chang A, Ferraro R, Xie P, Janowiak J, Rudolf B, Schneider U, Curtis S, Bolvin D, Gruber A, Susskind J, Arkin P (2003) The Version 2 global precipitation climatology project (GPCP) monthly precipitation analysis (1979–Present). J Hydrometeor 4:1147–1167

Alexander M, Bhatt U, Walsh J, Timlin M, Miller J, Scott J (2004) The atmospheric response to realistic Arctic sea ice anomalies in an AGCM during winter. J Clim 17:890–905

Baldwin MP, Dunkerton TJ (2001) Stratospheric harbingers of anomalous weather regimes. Science 294:581

Baldwin MP, Thompson DWJ (2009) A critical comparison of stratosphere-troposphere coupling indices. Q J R Meteorol Soc 135:1661–1672

Ballinger TJ, Allen MJ, Rohli RV (2014) Spatiotemporal analysis of the January Northern Hemisphere circumpolar polar vortex over the contiguous United States. Geophys Res Lett. doi:10.1002/2014GL060285

Barnes EA (2013) Revisiting the evidence linking Arctic amplification to extreme weather in midlatitudes. Geophys Res Lett 40:4728–4733. doi:10.1002/grl.50880

Bjerknes J (1964) Atlantic air-sea interaction. Adv Geophys 10:1–82

Brönnimann S (2007) Impact of El Niño-Southern Oscillation on European climate. Rev Geophys 45:RG3003. doi:10.1029/2006RG000199

Cassou C (2008) Intraseasonal interaction between the Madden-Julian oscillation and the North Atlantic oscillation. Nature 455(7212):523–527. doi:10.1038/nature07286

Cellitti MP, Walsh JE, Rauber RM, Portis DH (2006) Extreme cold air outbreaks over the United States, the polar vortex, and the large-scale circulation. J Geophys Res 111:D02114. doi:10.1029/2005JD006273

Cohen J, Barlow M, Kushner PJ, Saito K (2007) Stratosphere-troposphere coupling and links with Eurasian land surface variability. J Clim 20:5335–5343

Cohen JL, Furtado JC, Barlow MA, Alexeev VA, Cherry JE (2012) Arctic warming, increasing snow cover and widespread boreal winter cooling. Environ Res Lett 7:014007

Collins M, Knutti R, Arblaster J, Dufresne J-L, Fichefet T, Friedlingstein P, Gao X, Gutowski WJ, Johns T, Krinner G, Shongwe M, Tebaldi C, Weaver AJ, Wehner M (2013) Long-term climate change: projections, commitments and irreversibility. In: Stocker TF, Qin D, Plattner G-K, Tignor M, Allen SK, Boschung J, Nauels A, Xia Y, Bex V, Midgley PM (eds) Climate Change 2013: The physical science basis contribution of working group I to the fifth assessment report of the intergovernmental panel on climate change. Cambridge University Press, Cambridge

Czaja A, Frankignoul C (1999) Influence of the North Atlantic SST on the atmospheric circulation. Geophys Res Lett 26:2969–2972

Deser C, Tomas RA, Peng S (2007) The transient atmospheric circulation response to North Atlantic SST and sea ice anomalies. J Clim 20:4751–4767

Deser C, Phillips AS, Alexander MA (2010) Twentieth Century Tropical Sea Surface Temperature Trends Revisited. Geophys Res Lett 37:L10701. doi:10.1029/2010GL043321

Douville H (2009) Stratospheric polar vortex influence on Northern Hemisphere winter climate variability. Geophys Res Lett 36:L18703. doi:10.1029/2009GL039334

Drevillon M, Cassou C, Terray L (2003) Model study of the North Atlantic region atmospheric response to autumn tropical atlantic sea-surface-temperature anomalies. Quart J Roy Meteorol Soc 129:2591–2611. doi:10.1256/qj.02.17

Duchon CE (1979) Lanczos filtering in one and two dimensions. J Appl Meteor 18:1016–1022. doi:10.1175/1520-0450(1979)018<1016:LFIOAT>2.0.CO;2

Eden C, Jung T (2001) North Atlantic interdecadal variability: Oceanic response to the North Atlantic Oscillation (1865–1997). J Clim 14:676–691

Fischer EM, Luterbacher J, Zorita E, Tett SFB, Cast C, Wanner H (2007) European climate response to tropical volcanic eruptions over the last half millennium. Geophys Res Lett 34:L05707. doi:10.1029/2006GL027992

Fletcher CG, Hardiman SC, Kushner PJ, Cohen J (2009) The dynamical response to snow cover perturbations in a large ensemble of atmospheric GCM integrations. J Clim 22:1208–1222

Francis J, Vavrus S (2012) Evidence linking Arctic amplification to extreme weather in mid-latitudes. Geophys Res Lett 39:L06801. doi:10.1029/2012GL051000

Francis J, Chen W, Leathers D, Miller J, Veron D (2009) Winter Northern Hemisphere weather patterns remember summer Arctic sea ice extent. Geophys Res Lett 36:L07503. doi:10.1029/2009GL037274

Gill AE (1980) Some simple solutions for heat-induced tropical circulation. Q J R Meteorol Soc 106:447–462. doi:10.1002/qj.49710644905

Gray LJ, Scaife AA, Mitchell DM, Osprey S, Ineson S, Hardiman S, Butchart N, Knight J, Sutton R, Kodera K (2013) A lagged response to the 11 year solar cycle in observed winter Atlantic/European weather patterns. J Geophys Res Atmos 118:13405–13420. doi:10.1002/2013JD020062

Guirguis K, Gershunov A, Schwartz R, Bennett S (2011) Recent warm and cold daily winter temperature extremes in the Northern Hemisphere. Geophys Res Lett 38:L17701. doi:10.1029/2011GL048762

Gulev SK, Latif M, Keenlyside N, Park W, Koltermann KP (2013) North Atlantic Ocean control on surface heat flux on multidecadal timescales. Nature 499:464–467

Honda M, Inoue J, Yamane S (2009) Influence of low Arctic sea ice minima on anomalously cold Eurasian winters. Geophys Res Lett 36:L08707. doi:10.1029/2008GL037079

Horel JD, Wallace JM (1981) Planetary-scale atmospheric phenomena associated with the Southern Oscillation. Mon Wea Rev 109:813–829

Hoskins BJ, James IN, White GH (1983) The shape, propagation and mean-flow interaction of large-scale weather systems. J Atmos Sci 40:1595–1612

Hurrell J, van Loon WH (1997) Decadal variations in climate associated with the North Atlantic Oscillation. Clim Change 36:301–326

Ineson S, Scaife AA, Knight JR, Manners JC, Dunstone NJ, Gray LJ, Haigh JD (2011) Solar forcing of winter climate variability in the Northern Hemisphere. Nat Geosci 4:753–757

Jung T, Vitart F, Ferranti L, Morcrette J-J (2011) Origin and predictability of the extreme negative NAO winter of 2009/10. Geophys Res Lett 38:L07701. doi:10.1029/2011GL046786

Kalnay et al (1996) The NCEP/NCAR 40-year reanalysis project. Bull Am Meteor Soc 77:437–470

Kang D, Lee M-I, Im J, Kim D, Kim H-M, Kang H-S, Schubert SD, Arribas A, MacLachlan C (2014) Prediction of the Arctic Oscillation in boreal winter by dynamical seasonal forecasting systems. Geophys Res Lett 41:3577. doi:10.1002/2014GL060011

Kavvada A, Ruiz-Barradas A, Nigam S (2013) AMO's structure and climate footprint in observations and IPCC AR5 climate simulations. Clim Dyn. doi:10.1007/s00382-013-1712-1

Kerr RA (2000) A North Atlantic climate pacemaker for the centuries. Science 288(5473):1984–1986

Kitoh A, Arakawa O (1999) On overestimation of tropical precipitation by an atmospheric GCM with prescribed SST. Geophys Res Lett 26:2965–2968

Kumar A et al (2010) Contribution of sea ice loss to Arctic amplification. Geophys Res Lett 37:L21701. doi:10.1029/010GL045022

Kushnir Y, Robinson WA, Bladé I, Hall NMJ, Peng S, Sutton R (2002) Atmospheric GCM Response to Extratropical SST Anomalies: synthesis and Evaluation. J Clim 15:2233–2256

Liu J, Curry JA, Wang H, Song M, Horton RM (2012) Impact of declining Arctic sea ice on winter snowfall. PNAS. doi:10.1073/pnas.1118734109

Losada T, Rodriguez-Fonseca B, Mechoso CR, Ma H-Y (2008) Impact of SST anomalies on the North Atlantic atmospheric circulation : a case study for the northern winter 1995–1996. Clim Dyn 29:807–819

Magnusdottir G, Deser C, Saravanan R (2004) The effects of North Atlantic SST and sea ice anomalies on the winter circulation in CCM3, Part I: main features and storm-track characteristics of the response. J Clim 17:857–876

Maidens A, Arribas A, Scaife AA, MacLachlan C, Peterson D, Knight J (2013) The influence of surface forcings on prediction of the north atlantic oscillation regime of winter 2010/11. Mon Wea Rev 141:3801–3813. doi:10.1175/MWR-D-13-00033.1

Msadek R, Frankignoul C, Li L (2011) Mechanisms of the atmospheric response to North Atlantic multidecadal variability: a model study. Clim Dyn 36:1255–1276

Neale RB et al (2011) Description of the NCAR Community Atmosphere Model (CAM5). National Center for Atmospheric Research Tech. Rep. NCAR/TN-486+STR, p 268

Okumura Y, Xie SP, Numaguti A, Tanimoto Y (2001) Tropical Atlantic air-sea interaction and its influence on the NAO. Geophys Res Lett 28:1507–1510

Omrani NE, Keenlyside NS, Bader J, Manzini E (2014) Stratosphere key for wintertime atmospheric response to warm Atlantic decadal conditions. Clim Dyn 42:649–663

Peings Y, Magnusdottir G (2014a) Response of the wintertime northern hemisphere atmospheric circulation to current and projected Arctic Sea ice decline: a numerical study with CAM5. J. Climate 27:244–264

Peings Y, Magnusdottir G (2014b) Forcing of the wintertime atmospheric circulation by the multidecadal fluctuations of the North Atlantic ocean. Environ Res Lett 9(3):034018

Peings Y, Saint-Martin D, Douville H (2012) A numerical sensitivity study of the Siberian snow influence on the northern annular mode. J Clim 25:592–607

Peng S, Robinson WA, Li S (2002) North Atlantic SST Forcing of the NAO and relationships with intrinsic hemispheric variability. Geophys Res Lett 29(8):117. doi:10.1029/2001GL014043

Peng S, Robinson WA, Li S, Hoerling MP (2005) Tropical Atlantic SST forcing of coupled north atlantic seasonal responses. J Clim 18(3):480–496. doi:10.1175/JCLI-3270.1

Peterson TC, Hoerling MP, Stott PA, Herring S (2013) Explaining extreme events of 2012 from a climate perspective. Bull Am Meteor Soc 94(9):1–74

Petoukhov V, Semenov V (2010) A link between reduced Barent-Kara sea ice and cold winter extremes over northern continents. J Geophys Res 115:D21111. doi:10.1029/2009JD013568

Rayner NA, Parker DE, Horton EB, Folland CK, Alexander LV, Rowell DP, Kent EC, Kaplan A (2003) Global analyses of sea surface temperature, sea ice, and night marine air temperature since the late nineteenth century. J Geophys Res 108(D14):4407. doi:10.1029/2002JD002670

Scaife AA et al (2014) Skillful long- range prediction of European and North American winters. Geophys Res Lett 41:2514–2519. doi:10.1002/2014GL059637

Screen JA, Simmonds I (2013) Exploring links between Arctic amplification and mid-latitude weather. Geophys Res Lett 40:959. doi:10.1002/grl.50174

Screen JA, Simmonds I, Deser C, Tomas R (2013) The atmospheric response to three decades of observed Arctic sea ice loss. J Clim. doi:10.1175/JCLI-D-12-00063.1

Semmler T, McGrath R, Wang S (2012) The impact of Arctic sea ice on the Arctic energy budget and on the climate of the Northern mid-latitudes. Clim Dyn (EC-Earth Special Issue). doi: 10.1007/s00382-012-1353-9

Serreze M, Barrett A, Stroeve J (2009) The emergence of surface-based Arctic amplification. Cryosphere 3:11–19

Slingo J (2013) Why was the start to spring 2013 so cold? Metoffice, http://www.metoffice.gov.uk/media/pdf/i/2/March2013.pdf

Tang Q, Zhang X, Yang X, Francis JA (2013) Cold winter extremes in northern continents linked to Arctic sea ice loss. Environ Res Lett 8:014036

Thompson DWJ, Wallace JM (1998) The Arctic Oscillation signature in the wintertime geopotential height and temperature fields. Geophys Res Lett 25:1297–1300

Toniazzo T, Scaife AA (2006) The influence of ENSO on winter North Atlantic climate. Geophys Res Lett 33:L24704. doi:10.1029/2006GL027881

Trenberth KE, Fasullo JT, Branstator G, Phillips AS (2014) Seasonal aspects of the recent pause in surface warming. Nat Clim Change. doi:10.1038/nclimate2341

Vautard R (1990) Multiple weather regimes over the North Atlantic: analysis of precursors and successors. Mon Wea Rev 118:2056–2081. doi:10.1175/1520-0493(1990)118<2056:MWROTN>2.0.CO;2

Vihma T (2014) Effects of Arctic Sea ice decline on weather and climate: a review. Surv Geophys. doi:10.1007/s10712-014-9284-0

Wallace JM, Held IM, Thompson DWJ, Trenberth KE, Walsh JE (2014) Global warming and winter weather. Science 343(6172):729–730. doi:10.1126/science.343.6172.729

Waugh DW, Polvani LM (2010) Stratospheric polar vortices. In: LM Polvani, AH Sobel, DW Waugh (eds) The stratosphere: dynamics, transport and chemistry. American Geophysical Union, Washington, DC

Xie S-P, Carton JA (2004) Tropical atlantic variability: patterns, mechanisms, and impacts. In: Wang C, Xie SP, Carton JA (eds) Earth's climate. American Geophysical Union, Washington, DC. doi:10.1029/147GM07